UNIVERSITY OF THESSALY

SCHOOL OF ENGINEERING

DEPARTMENT OF ELECTRICAL AND COMPUTER ENGINEERING

ANTENNA ANALYSIS IN MILLIMETER WAVELENGTHS FOR 5G APPLICATIONS

Diploma Thesis

GEORGIOS ADAMAKIS

Supervisor: EVMORFOPOYLOS NESTOR

Volos 2020

UNIVERSITY OF THESSALY

SCHOOL OF ENGINEERING

DEPARTMENT OF ELECTRICAL AND COMPUTER ENGINEERING

ANTENNA ANALYSIS IN MILLIMETER WAVELENGTHS FOR 5G APPLICATIONS

Diploma Thesis

GEORGIOS ADAMAKIS

Supervisor: EVMORFOPOYLOS NESTOR

Volos 2020

ΠΑΝΕΠΙΣΤΗΜΙΟ ΘΕΣΣΑΛΙΑΣ
ΠΟΛΥΤΕΧΝΙΚΗ ΣΧΟΛΗ
ΤΜΗΜΑ ΗΛΕΚΤΡΟΛΟΓΩΝ ΜΗΧΑΝΙΚΩΝ ΚΑΙ ΜΗΧΑΝΙΚΩΝ ΥΠΟΛΟΓΙΣΤΩΝ

ΑΝΑΛΥΣΗ ΚΕΡΑΙΩΝ ΣΕ ΜΙΛΛΙΜΕΤΡΙΚΑ ΜΗΚΗ ΚΥΜΑΤΟΣ ΓΙΑ ΕΦΑΡΜΟΓΕΣ 5G

Διπλωματική Εργασία

ΓΕΩΡΓΙΟΣ ΑΔΑΜΑΚΗΣ

Επιβλέπων/πουσα: ΕΥΜΟΡΦΟΠΟΥΛΟΣ ΝΕΣΤΩΡ

Βόλος 2020

Approved by the Examination Committee:

Supervisor **EVMORFOPOYLOS NESTOR**
Assistant Professor, Department of Electrical and Computer Engineering, University of Thessaly

Member **Stamoulis Georgios**
Professor, Electrical and Computer Engineering, University of Thessaly

Member **Plessa Fotios**
Associate Professor, Electrical and Computer Engineering, University of Thessaly

Acknowledgements

I would like to thank my supervisor, Mr Nestor Evmorfopoulos for trusting in writing this thesis.

DISCLAIMER ON ACADEMIC ETHICS AND INTELLECTUAL PROPERTY RIGHTS

«Being fully aware of the implications of copyright laws, I expressly state that this diploma thesis, as well as the electronic files and source codes developed or modified in the course of this thesis, are solely the product of my personal work and do not infringe any rights of intellectual property, personality and personal data of third parties, do not contain work / contributions of third parties for which the permission of the authors / beneficiaries is required and are not a product of partial or complete plagiarism, while the sources used are limited to the bibliographic references only and meet the rules of scientific citing. The points where I have used ideas, text, files and / or sources of other authors are clearly mentioned in the text with the appropriate citation and the relevant complete reference is included in the bibliographic references section. I also declare that the results of the work have not been used to obtain another degree. I fully, individually and personally undertake all legal and administrative consequences that may arise in the event that it is proven, in the course of time, that this thesis or part of it does not belong to me because it is a product of plagiarism».

The declarant

GEORGIOS ADAMAKIS

Abstract

The field of Telecommunication is in a rapid growth the last decades, with the past ten years being very important for the corresponding technologies. Every decade, a new generation of wireless communication is being born. In the current thesis I refer to the antennas of the 5^{th} generation, which are a significant part of the whole evolution. In order to do so, one must comprehend the theory behind the antennas, as well as what is actually an antenna. Also, as the electromagnetic spectrum is becoming more congested, the frequency band of mm wave lengths offers a lot of advantages for the future wireless communications like 5G, however there and notable drawbacks. Maxwell's equations help us see through the electomagnetic waves and their properties, while they are a key point for the development of other theories like the microwave circuits and transmission line theory, which are of the same significance for the purpose of this thesis. In addition, different antenna parameters will help us describe the function of those structures. I will focus on the omnidirectional antennas like microstrip or patch antenna, as they can be part of the so called phased arrays, a kind of smart antennas. Phased arrays have the ability to create narrow beams and steer them to the direction an operator wishes, thus they are suited 5G antennas functioning at mm-wave band frequencies. In the final sections, what was previously described is depicted with the help of simulation tools and scripts. Digital simulations have the advantage that we can see how a theory is applied, without the need of material parts, except from a computer, consequently saving time and money. Thanks to such tools the evolution of Telecommunications and other engineering fields are passing to a new era, helping the needs of people and creating new opportunities.

Περίληψη

Ο κλάδος των τηλεπικοινωνιών βρίσκεται σε ταχείς ρυθμούς ανάπτυξης τις τελευταίες δεκαετίες, με τα τελευταία δέκα χρόνια να παίζουν κομβικό ρόλο. Στη παρούσα διπλωματική εργασία αναφέρομαι στις κεραίες της 5ης γεννιάς τηλεπικοινωνιών, οι οποίες αποτελούν σημαντικό κομμάτι της συνολικής εξέλιξης των συστημάτων. Για να επιτευχθει αυτός ο σκοπός, χρειάζεται να κατανοηθεί η θεωρία των κεραιών οπώς επίσης τι είναι ουσιαστικά το στοιχείο της κεραίας. Συνεχίζοντας, καθώς το ηλεκτρομαγνητικό φάσμα επικοινωνιών είναι πλέον αρκετά συνωστισμένο, το φάσμα συχνοτήτων των μιλλιμετρικού (*μμ*) μήκους κύματος προσφέρει αρκετά πλεονεκτήματα για τις μελλοντικές ασύρματες επικοινωνίες όπως το 5G, με αντιληπτά μειονεκτήματα παρόλα αυτά. Οι εξισώσεις του Maxwell μας βοηθάνε να κατανοήσουμε την διάδωση και τις ιδιότητες των ηλεκτρομαγωνητικών κυμάτων, ενώ παράλληλα αποτελούν έναυσμα για θεωρίες όπως μικροκυμματικά κυκλώματα και γραμμές μεταφοράς, εργαλεία που είναι σημαντικά για την ανάπτυξη της παρούσας εργασίας. Επιπρόσθετα, διάφορες παράμετροι των κεραιών θα βοηθήσουν στην κατανόηση της λειτουργίας αυτών των συστημάτων. Θα εστιάσω στις πανκατευθυντικές κεραίες, όπως οι *microstrip* ή *patch* κεραίες, καθώς με αυτές μπορούν να αποτελέσουν κομμάτι μιάς συστοιχίας κεραιών, ή αλλίως μέρος σύγχρονων ”έξυπνων” κεραιών. Μία τέτοια δομή έχει την ικανότητα να δημιουργεί μία στενόμακρη ακτινοβολία, η οποία είναι δυνατό να κατευθύνεται προς το σημείο το οποίο επιθυμεί ένας χειριστής και κατα συνέπεια να είναι αρκετά κατάλληλες για κεραίες της 5ης γεννιάς στα *μμ* μήκη κύματος. Στο τελευταίο μέρος της διπλωματικής, για ότι περιγράφηκε προηγουμένως, υπάρχουν ενδεικτικές προσομοιώσεις μέσω αντίστοιχων εργαλείων και προγραμματισμού. Η ψηφιακή προσομοίωση φαινομένων βοηθάει να κατανοήσουμε το πως εφαρμόζεται η θεωρία, χρησιμοποιώντας απλά έναν υπολογιστή, εξοικονομώντας χρόνο και χρήματα. Χάρις αυτά τα εργαλεία οι Τηλεπικοινωνίες και γενικότερα ο κόσμος της μηχανικής εξελίσεται ταχύτατα, με σκοπό της βελτίωση των ζωών και των αναγκών μας.

Table of contents

List of figures

List of tables

Abbreviations

2D	2-dimensional
3D	3-dimensional
3GPP	3rd Generation Partnership Project
AI	Artificial Intelligence
AMPS	Advanced Mobile Phone Service
BW	Bandwidth
EM	Electromagnetic
FM	Frequency Modulation
GPS	Global Positioning System
GSM	Global System for Mobile Telecommunications
HPBW	Half Power Beam width
IC	Integrated Circuit
ITC	Information and Communications Technology
ITU	International Telecommunication Union
LTE	Long Term Evolution
MIMO	Multiple-input and Multiple-output
MSA	Microstrip Antenna
MoM	Method of Moments
PCB	Printed Circuit Board
SMS	Short Message Service
TEM	Transverse Electromagnetic
UE	User Equipment
VNA	Vector Network Analyzer
WiMAX	Worldwide Interoperability for Microwave Access
db	decibel

mMIMO	massive Multiple-input and Multiple-output
mm	millimeter
w.r.t	with respect to

Chapter 1

Introduction

The field of telecommunication and wireless cellular systems, along with other computer science technologies, are being grown in a rapid way the last decade. New solutions and advancements are created every year, walking towards the the future, to the era of the 4^{th} Industrial Revolution. Wireless telecommunication systems are in the center of research as the need for more data and speed combined with the number of human and non-human devises getting increased, has become a mandatory factor. Thus, the emerging technology of 5G systems plays a major role, as they fulfil the requirements described previously but also, they will open new perspectives in the fields of communication and industry.

1.1 Thesis Subect

The purpose of this thesis is to introduce the concept of antennas and wireless cellular systems, unfolding the theoretical concepts behind those infrastructures, and then go deeper, analysing the subject in more detail. More specific, the future of those systems depends on the future mm-Wave antennas, which are suited for the next generation of wireless systems and particularly the 5^{th} generation or 5G.

Two main advantages of these structures has to do with the ability steer the beam to the direction we want, while operating at higher frequencies, the bandwidth increases too. In other words, when a user for example is located somewhere in the city, the antenna can directly send the beam to his/her direction. Also, higher bandwidth means improved data rates, enabling new application to exist on a moving user. However, a few problems emerge. The first one concerns the fact that an EM wave at such small wavelengths is easily fading or blocked

due to weather conditions or intermediate obstacles. Furthermore, 5G system might not be compatible with the already existing base stations or devices, thus, the deployment in a large scale should cost money and time.

1.1.1 Contribution

The contribution of the thesis is summarized as:

1. A study on the omnidirectional antennas
2. Connection of them with microwave circuits which propagate EM waves
3. Phased array formation with K identical elements placed linearly
4. Tapering methods which affect quantity measures of the antennas
5. Python simulation to comprehend and visualize the theoretical methods

1.2 Chapter synopsis

The thesis consists of 5 chapters. In chapter 2 there is a brief history reference about the origins of wireless communications and how they have evolved through the centuries, reaching the modern systems. In chapter 3 someone can see how through Maxwell's equations an antenna is functioning, basic antennas structures and parameters, a study on microwave circuits and transmission lines and the microstrip-patch antenna. Going to chapter 4 I introduce the concept of linear phased arrays and the affect of mutual coupling. Finally, chapter 5 we can see some simulations of phased arrays and measures regarding their basic parameters.

Chapter 2

History

2.1 People and communication

Communication is the exchange of information among living beings, information that is important for each participant, making communication a vital and significant act. In the ancient years, different civilizations and cities started developing their own products, which by the development of trade procedure and the means of transport, started traveling among all those destinations. Side by side with the products, information was also able to get from one point to another. As the centuries passed, new ways and ideas evolved, such as letters, books, newspapers that could be transferred through trains or ships. Simultaneously, sciences like mathematics and physics were rapidly developed, especially the 19^{th} and 20^{th} centuries, and in this way the concepts of wireless communication and Telecommunications were born changing dramatically the conception of information's "journey". An alternative of a mean was given, more specific signals traveling through the air.

The person behind the significant alter of the communications was the famous physicist Heinrich Hertz. He was working as a Professor at the Technical Institute in Karlsruhe and in 1886 made the first complete radio system. A transmitter antenna produced sparks at a gap and the sparking occurred at a gap of the receiving antenna, as shown at the figure 2.1 [1]. In fact, what Hertz did, was to prove the theoretical assumption of James Clerk Maxwell about the existence of electromagnetic waves, which were predicted through the well-known Maxwell's equations. Some decades later another scientist, not so popular, developed the first practical radio system. Guglielmo Marconi, who came from Italy, had become obsessed with the idea of sending messages through a wireless communication system and was the first to

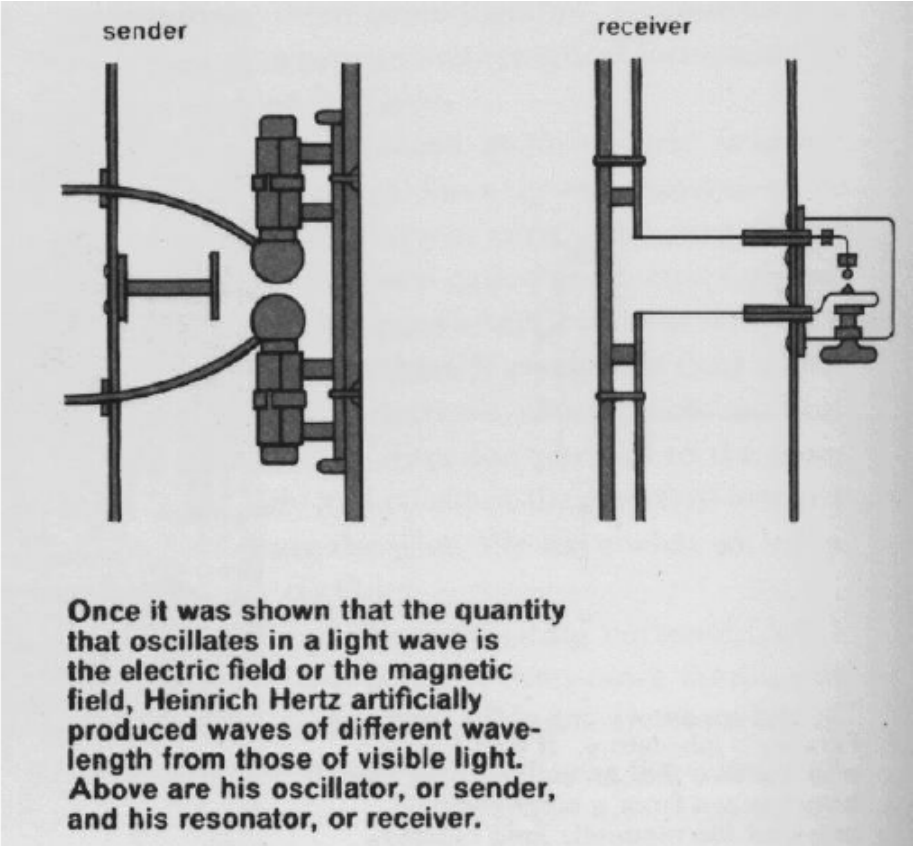

Figure 2.1: First radio system of Heinrich Hertz operating at a wavelength of about 8 meter [1]

create such a system that could perform across the Atlantic Ocean.

2.2 Antennas

It has become clear from the previous section that the key element for the wireless communication is the antenna. With simple words:

Definition 2.1. *Antenna is usually metallic device (such as a rod or wire) for radiating or receiving radio waves [4].*

Antennas come in many sizes and shapes depending on their purpose. Some of the most common are:

- Dipole antenna
- Thin wire antenna
- Reflector antanna

- Horn antenna
- Microstrip or patch antenna

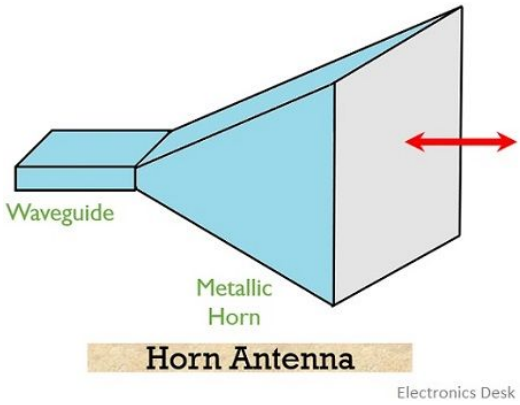

(α□) Horn antenna [8]

(β□) Reflector antenna [9]

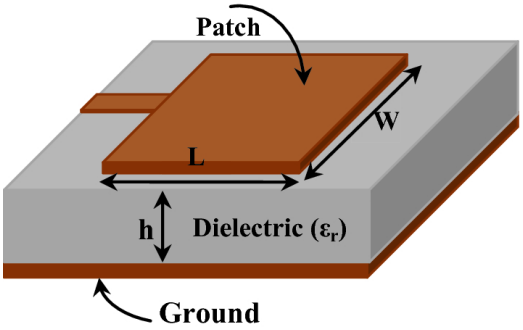

(γ□) Microstrip Antenna [10]

Figure 2.2: Types of antennas

The last century, there has been a vast use of those elements for the sake of communications. Marconi's antennas, referred in the previous section, were wire antennas of relatively large size (60 meters) and were built onto two wooden poles. Due to their inefficiency, there was the need for a lot of power and as a result sometimes they glowed during the night. Nowadays,

wire antennas are used for the reception of radio signals for cars or portable devices. Another kind, reflector antennas are commonly deployed for satellite television. On the long list of antenna elements and what each purpose they serve, next there are the so called microstrip antennas and phased arrays. Microstrip antennas are printed metal structures on a substrate, or in other words they are a kind of PCBs (Printed-Circuit-Board) [4]. Generally printed antennas are used today for smartphones and more recently they have been realized on chips in integrated circuits (ICs) [11]. The need for analyzing microstrip or patch antennas is that these elements can be part of the phased arrays.

Phased arrays are a composition of immovable antennas. More specific, by combining a large number of small antennas, which are described by low antenna gain, then a phased array is created. Those small radiating components could be microstrip or dipole antennas. Phased arrays can be characterized as smart antennas as they are able to steer their main lobe to the desired direction. This is achieved by electronically setting specific amplitudes and phases at each element, thus getting the name of Phased Array. At their initial deployment, between 1970 and 1990, military made use of them in order to replace the mechanically steering antennas of their radars. Apart from military purposes, in the present phased arrays are also found at radio astronomy and play a key role at future telecommunications. The reason to chose phased arrays at telecommunication system evolution is not only their ability of steering the beam but also the property of establishing constant and simultaneous communicative links. What is meant by future TELECOM is the upcoming era of the 5G.

2.3 Wireless communications

Broadly the concept of sending signals through the air, without the use of physical medium can be described with the words of Wireless Communications. Cellular systems are a nice example and they have been deployed for Telecommunications since the 1950. The last decades, a new cellular system emerges every ten years with the 5G (5^{th} Generation) being the most recent and very promising. But first let us take a look at some previous generation systems.

- 1G: Was an analogue type of system, voice-centric. It was developed in the year of 1983, and it used FM radios. At the time digital radio systems were expensive so analogue systems were preferable. In the USA this system was named AMPS (Advanced

Mobile Phone Service)

- 2G: The evolution from 1G to 2G also meant the change from analogue to digital. From 1990 to 1997 2G was named GSM (Global System for Mobile Communications) while USA and Korea were developing the IS-95. At this point the idea of SMS (Short Message Service) was introduced

- 3G: As the previous systems were voice-centric the pass to the 3G introduced the idea of data-centric communications. It was the first international standard that was released by the ITU (International Telecommunication Union) in 1999. 3G networks penetrated in Japan, USA and Europe in 2008 over 100

- 4G: Approaching the modern times since 2013 4G is being used most cellular systems. 3G introduced the idea of data and internet, now 4G comes with much higher data speeds, shifting to the era of mobile applications and mobile video. In Europe and in many other countries major cellular operators prefer the LTE (Long Term Evolution) system while USA had already developed WiMAX (Worldwide Interoperability for Microwave Access). WiMAX is based on the Wi-fi technology. Both LTE and WiMAX systems are very similar [12]

Having described the cellular systems through the decades it is time to introduce the 5th Generation of these systems. The initial steps are placed in 2010 and the first large-scale projects were METIS and 5GNow, that launched 2 years later [13]. The International Telecommunications Union (ITU) has defined the requirements that 5G has to meet to be chosen as an official International Mobile Telecommunications 2020 (IMT - 2020) technology and published related evaluation guidelines [12]. On the way towards the fulfilment of the IMT-2020 framework, the standardization of an early phase of 5G New Radio by the 3rd Generation Partnership Project (3GPP) is in full swing. Although 5G has been commercially deployed since 2019 in many countries (Europe, USA, Asia), pre-commercial deployments have already existed such as the at Olympics of Tokyo and Winters Olympics of South Korea, as well as at EURO 2020. 5G is not just an evolution of the 4G or previous technologies, but a completely different alteration in Telecommunications. As a revolutionary technology 5G shall unleash new perspectives leading to human-centric and machine-centric applications. In that manner the impact on society and industry will be huge reaching beyond the Information and Communications Technology (ITC). The last decade it is estimated that global mobile

traffic has increased 1000x and that is because the need for data-driven services of smart phones has significantly increased. Main reasons are the social networks, multimedia applications, augmented reality etc. In the same manner, another factor is that the number of connected devises also create a problem. Apparently, the mass connection of data-hungry human and non-human devises imposes the great challenges that 5G and future cellular infrastructures will face. Consequently, as the stages for the global establishment of the new age cellular systems go forward, here are some cases of what it is expected [13]:

1. The critical passage to the age of the 4th Industrial revolution or Industrial 4.0. The advancement of AI combined with the reliable and low-latency communications will enable the machine-to-machine or machine-to-human communications in general, but also at industrial environments

2. Similarly, will play a key role at automotive and transport sector by providing safety and efficiency to the existing and coming means of transport

3. Provide remote control service for machines or sites that are dangerous or inaccessible, like construction fields

4. A next step for health services through the possibility of wirelessly enabled smart Pharmaceuticals or remote surgery with haptic feedback

5. Smart cities and smart housing, by the improving everyday life with energy and waste management and better transportation

Chapter 3

Antenna Theory

3.1 Antenna Parameters

3.1.1 Spherical coordinates and Time-Harmonic fields

In order to describe the parameters of an antenna it is essential to define the coordinate system that is needed. Antennas, generally are located at the center of the coordinate system and propagate EM waves to outer directions. For this case, spherical coordinates can help get a better analysis, so the set of *r*, θ and φ is suitable. In addition, we assume that the all the currents and fields have a sinusoidal time variation. The electric field (3.2) is given by a complex function (3.1) as is seen below:

$$\vec{E}(\vec{r}) = E_r(\vec{r})\vec{e}_r + E_\theta(\vec{\theta})\vec{e}_\theta + E_\phi(\vec{\phi})\vec{e}_\phi \tag{3.1}$$

$$\vec{\mathcal{E}}(\vec{r},t) = Re[\vec{E}(\vec{r})e^{j\omega t}]\cos(\omega t + \phi_0) \tag{3.2}$$

where $\omega = 2\pi f$ is the angular frequency, ϕ_0 is the phase of the complex field operating at a frequency f. More about the behaviour of the field and wave functions are shown in section 3.2.

3.1.2 Far field

An antenna placed at the origin of the coordinate system, generates EM waves that travel in free space. At this point, there can be distinguished three regions for the behaviour of the wave [4]:

1. Near-field region
2. Transition (*Fresnel*) - field region
3. Far-field region

At the third region, is where we find the so-called *plane waves* or *transverse electromagnetic waves* (TEM waves). They are defined as waves whose electric and magnetic components are perpendicular to each other but also, orthogonal to the direction of propagation [14]. They are usually spherical waves, as indicated in the previous paragraphs, that are locally flat.

3.1.3 Radiated Power - Poynting Vector

Suppose we have a wave at the frequency domain. When it is travelling in the far-field region, the power density that is radiated orthogonal to the magnetic and electric fields components, is called *Poynting vector* and it is measured in *Watts/square meter*. In other words:

Assume the field function $\vec{E}(\vec{r})$. According to theory the magnetic field is given by:

$$\vec{H}(\vec{r}) = \frac{1}{Z_0}\vec{e}_r \times \vec{E}(\vec{r})$$

. where $Z_0 = \sqrt{\frac{\mu_0}{\epsilon_0}} = 377\Omega$, with ϵ_0 the permittivity and μ_0 the permeability respectively. Poynting vector is given by the following equations:

$$\vec{S}_p(\vec{r}) = \frac{1}{2}Re[\vec{E}(\vec{r}) \times \vec{H}^*(\vec{r})]$$

or

$$\vec{S}_p(\vec{r}) = \frac{1}{2}Z_0^{-1}|\vec{E}(\vec{r})|^2\vec{e}_r$$

3.1.4 Radiation Pattern

Radiation pattern is one of the most important parameters of an antennas. It can be a function or a graphical representation (2D or 3D), that indicates the amount of energy that is radiated towards a certain direction. It must be mentioned that it is valid only in the far-field region. In order to define the radiation pattern, we must use the *Poynting vector* that was previously mentioned:

$$\vec{P}(\vec{r}) = \vec{P}(\theta, \phi) = |r^2\vec{S}_p(\vec{r})| \tag{3.3}$$

As it is seen by the equation, the function does not have a radial dependency, thus it is a measure showing the radiated power per solid angle. In addition, at certain values (θ_n, ϕ_n) the function has local maximas, from which there is a specific value referred as total maxima. The largest value is called *main lobe* and the other local maximas, if they exist, are called *sidelobes*. The structure of each element determines the existence of sidelobes and other factors concerning the way an antenna is radiating. Some examples are shown below at 3.1α and 3.1β

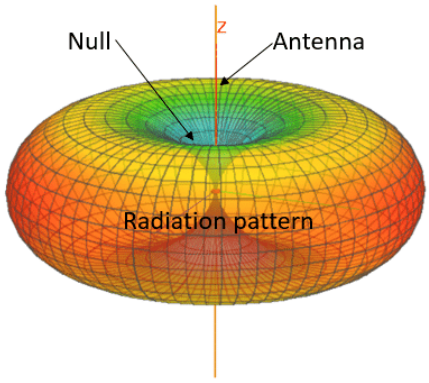

(α)

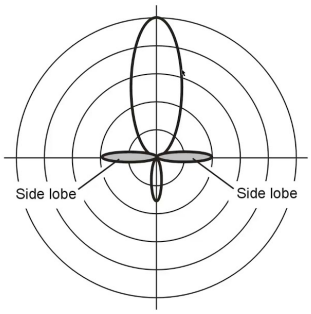

(β)

Figure 3.1: Radiation patterns (a) 3D pattern of a dipole antenna without sidelobes [2] (b) 2D pattern with sidelobes [3]

Thus, at the direction (θ_0, ϕ_0) radiation pattern reaches its maximum value. We can now introduce the measure of *Normalized radiation pattern*. Although, it cannot describe all the quality parameters of an antenna it is a useful function that will help determine other quality measures such as the gain or the directivity. It is given as:

$$F(\theta, \phi) = \frac{P(\theta, \phi)}{P(\theta_0, \phi_0)} \tag{3.4}$$

and is measured in dB using $10log_{10}(F(\theta, \phi))$. An example is shown at 3.2

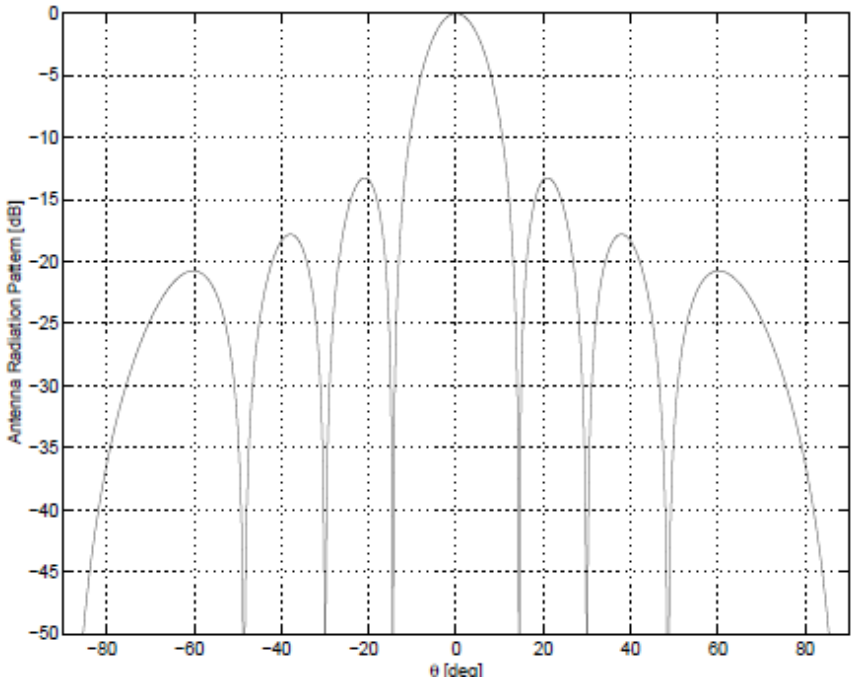

Figure 3.2: Normalized Radiation Pattern where main lobe is at the center (zeros degrees) and four sidelobes at other directions, measured in dB [4]

3.1.5 Directivity - Gain

It well known from antenna theory that an ideal element, that radiates equal energy to all direction does not exist. Such a hypothetical antenna is called *isotropic radiator* and is used in order to determine the factor of Directivity. Directivity describes the beamforming properties, meaning it depicts the concentration of power in the main lobe w.r.t other directions. It is referred as $D(\theta, \phi)$ and show the power density per solid angle.

For an isotropic radiator, with total power $P_t\ watts$, the equally distributed power density is given by $\frac{P_t}{4\pi}$. The function of directivity in general is:

$$D(\theta, \phi) = \frac{P(\theta, \phi)}{P_t/4\pi} \tag{3.5}$$

where $P(\theta, \phi)$(3.4) is the function of the radiation pattern and $D = max[D(\theta, \phi)]$ gives the maximum value of the equation (3.5).

When a feeder provides energy to the antenna, not all of this power ends up to the radiating

part, as there are losses due to the structure of the system. For example, ohmic losses or impedance-matching losses between the antenna and the transmission lines play an important role. In a similar manner, but now with the use of the total provided power P_{in}, we can define the gain of an antenna as:

$$G(\theta, \phi) = \frac{P(\theta, \phi)}{P_{in}/4\pi} \tag{3.6}$$

with $G = max[G(\theta, \phi)]$ the maximum of the gain. The relation of directivity and gain is given below as:

$$n = P_t/P_{in}$$

or

$$G = nD$$

where n is called *efficiency* of an antenna.

3.1.6 Half power beam width - Effective antenna aperture

A relevant parameter to the radiation pattern is the half power beam width or HPBW. Beam width is a parameter that indicates the concentration of radiating power to a certain area of the radiation pattern. More specific, at this region the radiated or received power is more than than the 50% ($-3db$) of the peak power. This area is expressed in angular metrics, in other words, there are two angles, θ_{HPBW} and ϕ_{HPBW} in the principle plane that show where more than the half power is concentrated. As it was mentioned before, HPBW is related to transmit and receive antennas.

An additional parameter, concerning the receiving antenna is the effective antenna aperture A_e. It defines the equivalent surface in which the antenna absorbs the incident electromagnetic field that is dissipated by the load impedance Z_L which is connected to the terminals of the antenna [4] and is given by:

$$A_e = \frac{P_r}{S_p} \tag{3.7}$$

where P_r is the power reaching the the load impedance and S_p the power density, which was mentioned previously. Effective antenna aperture is related with the property of gain with the

following equation:

$$G = \frac{4\pi A_e}{{\lambda_0}^2}$$

3.1.7 Polarization

When an antenna is designed, the polarization properties is an important parameter of the system, as it affects effectiveness of a signal reception. The radiated electric field, in the far-field region, has two components E_θ and E_ϕ, which are orthogonal to the direction that the wave is propagating. The relative phase difference, when represented in the frequency domain, of those components describe the way the antenna is polarized. According to antenna theory, function (3.8) depicts an ellipse in the plane, perpendicular to the direction of propagation, in which space-time dependence has been eliminated :

$$\left(\frac{\mathcal{E}_\theta}{E_1}\right)^2 + \left(\frac{\mathcal{E}_\phi}{E_2}\right)^2 - \frac{2\mathcal{E}_\theta\mathcal{E}_\phi}{E_1E_2}cos\phi = sin^2\phi \tag{3.8}$$

where

$$\mathcal{E}_\theta(\vec{r},t) = E_1(\vec{r})cos(\omega t - k_0 r)$$

and

$$\mathcal{E}_\phi(\vec{r},t) = E_2(\vec{r})cos(\omega t - k_0 r + \phi)$$

and ϕ the phase difference between the electric-field's components. In general, as mentioned previously, equation(3.8) is called *elliptical polarization*.For specific values applied at this equation, there can be two other kinds. First, if $E_1 = E_2 = E$ and $\phi = \pm\pi/2$ then we have the *circular polarization*: $\left(\frac{\mathcal{E}_\theta}{E_1}\right)^2 + \left(\frac{\mathcal{E}_\phi}{E_2}\right)^2 = 1$, which is the common circle equation. Second, if $E_1 \neq E_2$ and $\phi = \pm\pi$, it is called *linear polarization*: $\frac{\mathcal{E}_\theta}{E_1} + \frac{\mathcal{E}_\phi}{E_2} = 0$, in other words, an equation of a line. Figure 3.3 shows a graphical representation of the previous equations, regarding the plane and the propagation direction.

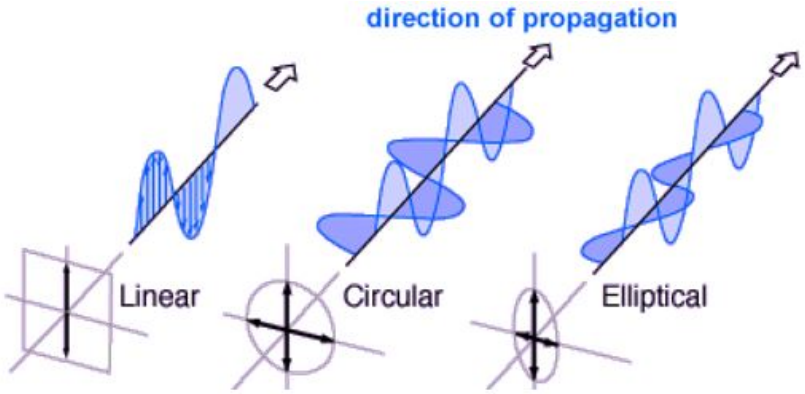

Figure 3.3: Kinds of polarization: (a)Linear (b)Circural (c)Elliptical [5]

3.2 Microwave circuits - Transmission Lines

When a EM wave is in the spectrum of *microwaves* or *millimeter-wave lengths* we need to apply the transmission line theory. These kind of waves correspond to frequencies ranging from $300MHz$ to $300GHz$ or in other words, according to the $c = \lambda f$ equation, wave lengths vary from $1m$ to $1mm$. In addition, when a physical component's dimension is a fraction of the wavelength, specifically more than 0.1λ, then transmission line theory is needed. For the purpose of this project, what we will focus on is the concept of *Microwave networks*.
Microwave networks consist of K ports connected to K transmission lines as seen in figure 3.4. These lines support TEM modes (transverse electromagnetic), meaning plane waves can propagate through them. In theory, the relation between the incident and reflected waves of currents and voltages, is given by the impedance matrix as seen below.

$$\begin{bmatrix} V_1 \\ . \\ . \\ V_K \end{bmatrix} = \begin{bmatrix} Z_{11} \, . \, . \, Z_{1K} \\ \cdots \\ \cdots \\ Z_{11} \, . \, . \, Z_{KK} \end{bmatrix} \begin{bmatrix} I_1 \\ . \\ . \\ I_K \end{bmatrix}$$

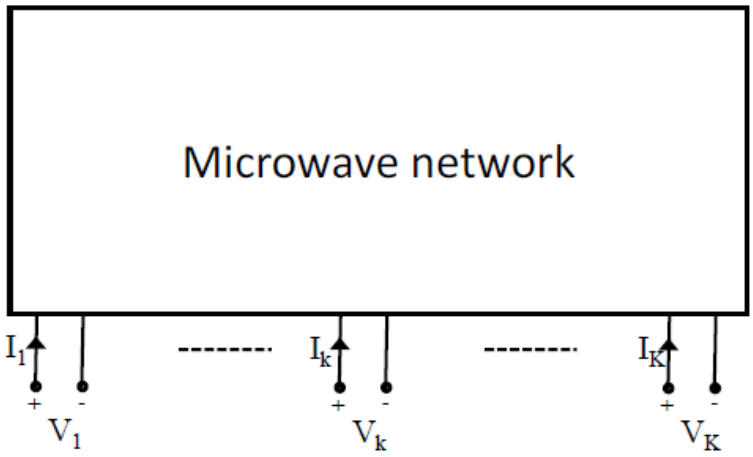

Figure 3.4: Representation of a K-port microwave network [4]

where $V_k = V_k^+ + V_k^-$, $I_k = I_k^+ - I_k^-$ with the notation $+/-$ meaning incident/reflected wave.

Despite the fact that impedance matrix offers a useful method to describe the network, at the desired frequencies it is not so practical, as we cannot measure precisely the complex values of the currents and voltages. What can be measured with less effort is the amplitude and phase of the incident and reflected electric field of the TEM wave. In order to achieve this, let's introduce another method, known as *Vector Network Analyzer* or just VNA. Now the complex incident and reflected wave amplitudes are normalized and are given as:

$$a_k = \frac{V_k^+}{\sqrt{Z_0}} = I_k^+ \sqrt{Z_0}$$

$$b_k = \frac{V_k^-}{\sqrt{Z_0}} = I_k^- \sqrt{Z_0}$$

where a_k is the incident wave and b_k the reflected. Usually in the measurements that will be needed the impedance Z_0 will be 50Ω. The relation of a_k and b_k is given with the help of a scattering matrix, which is given below for a K-port network.

$$\begin{bmatrix} b_1 \\ . \\ . \\ b_K \end{bmatrix} = \begin{bmatrix} S_{11} \, . \, . \, S_{1K} \\ \cdots \\ \cdots \\ S_{K1} \, . \, . \, S_{KK} \end{bmatrix} \begin{bmatrix} a_1 \\ . \\ . \\ a_K \end{bmatrix}$$

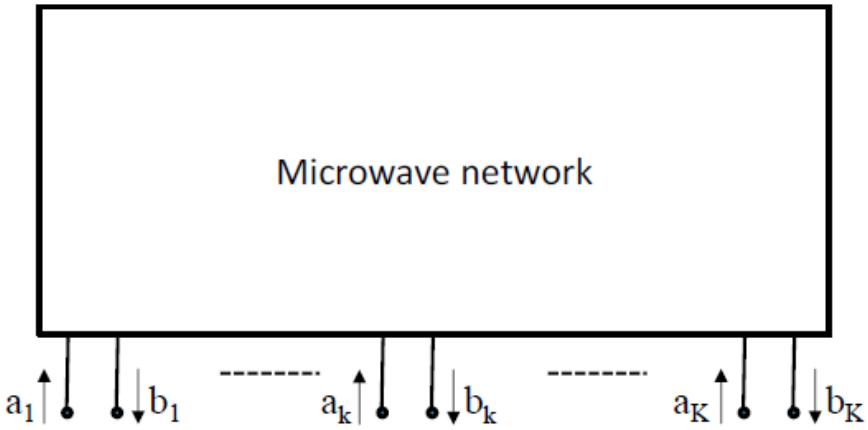

Figure 3.5: Representation of a K-port microwave network with normalized complex amplitudes [4]

Before explaining what the scattering matrix is, it is essential to describe the termination of a transmission line is and the impedance matching. Suppose there is a transmission line with characteristic impedance Z_0. The line is terminated by a load Z_L. The reflection coefficient is given as:

$$\Gamma = \frac{V_0^-}{V_0^+} = \frac{Z_L - Z_0}{Z_L + Z_0}$$

There are three cases according to this equation:

- $Z_0 = Z_L \Rightarrow \Gamma = 0$, matched load
- $Z_L = 0 \Rightarrow \Gamma = -1$, short circuit termination
- $Z_L = \infty \Rightarrow \Gamma = 1$, open circuit termination

When the load and characteristic impedances are matched, as is seen in the first case, then the maximum transfer power is ensured. Now, back to the scattering matrix or S-parameters, that is a method of describing the relation of incident and reflected power among the ports. For a set of ports the parameter S_{ij}, i is the port from which energy emerges and j the energy input port. In case of $i = j$, the element S_{ii} gives the reflected power at port i. In most cases, only one signal is injected at one port at one time. For an example of a 2-port networks, suppose there is a source port with Z_S impedance and a load port with Z_L impedance. S_{11} is the reflection coefficient, or the reflected energy at the source port and S_{22} the reflection at port 2 (load) respectively. S_{21} is the amount of power passed from the source to the load and

S_{12} the energy at the opposite direction. In addition, $|S_{21}|^2$ is called *forward gain* and $|S_{12}|^2$ *reverse gain*. The scattering parameters are given as:

- $S_{11} = \frac{b_1}{a_1}$, $a_2 = 0$
- $S_{21} = \frac{b_2}{a_1}$, $a_2 = 0$
- $S_{12} = \frac{b_1}{a_2}$, $a_1 = 0$
- $S_{22} = \frac{b_2}{a_2}$, $a_1 = 0$

3.3 Antennas and electormagnetic fields

3.3.1 Maxwell's equations

Maxwell's equation is the essential mathematical tool, which triggered the comprehension of electromagnetism. Specifically, the four famous equations, describe the way electric charges and currents create electric and magnetic fields. Maxwell's equations in the general form are:

$$\nabla \cdot E = \frac{\rho}{\epsilon_0}$$
$$\nabla \cdot B = 0$$
$$\nabla \times E = -\frac{\partial B}{\partial t}$$
$$\nabla \times B = \mu_0 \left(\boldsymbol{J} - \epsilon_0 \frac{\partial E}{\partial t} \right)$$

where E is the electric field, ρ is electric charge distribution, and $\boldsymbol{J}$ electric current distribution. Note that this symbolism is used general. In the next paragraphs there is going to be another way of describing the fields as there will be time and frequency domain fields.

Now, the current and charge distribution are found in a medium the equations take the following form, with time dependency:

$$\nabla \cdot \vec{\mathcal{D}}(\vec{r},t) = \vec{\rho}_e(\vec{r},t) \tag{3.9}$$

$$\nabla \cdot \vec{\mathcal{B}}(\vec{r},t) = 0 \tag{3.10}$$

$$\nabla \times \vec{\mathcal{E}}(\vec{r},t) = -\frac{\partial \vec{\mathcal{B}}(\vec{r},t)}{\partial t} \tag{3.11}$$

$$\nabla \times \vec{\mathcal{H}}(\vec{r},t) = \vec{\mathcal{J}}_e(\vec{r},t) + \frac{\partial \vec{\mathcal{D}}(\vec{r},t)}{\partial t} \tag{3.12}$$

where $\vec{\mathcal{D}}$ is the displacement current in C/m^2, $\vec{\rho}_e$ the electric charge distribution in C/m^3, $\vec{\mathcal{B}}$ the magnetic flux density in W/m^2, $\vec{\mathcal{E}}$ the electric field in V/m, $\vec{\mathcal{H}}$ the magnetic field in A/m and $\vec{\mathcal{J}}_e$ the electric current distribution in A/m^2. Another important equation, which is derived from Maxwell's theory is the continuity equation. It is a relation between charge and current distribution:

$$\nabla \cdot \vec{\mathcal{J}}_e(\vec{r},t) + \frac{\partial \vec{\rho}_e(\vec{r},t)}{\partial t} = 0 \tag{3.13}$$

As the medium of interest is antennas, propagating and receiving in the free space then:

$$\vec{\mathcal{D}}(\vec{r},t) = \epsilon_0 \vec{\mathcal{E}}(\vec{r},t)$$

$$\vec{\mathcal{H}}(\vec{r},t) = \mu_0 \vec{\mathcal{B}}(\vec{r},t)$$

We also, suppose there is a time-harmonic dependence for the fields, charges and distributions as mentioned in the beginning of the chapter, so now the dependence becomes angular, with frequency f and $\omega = 2\pi f$. For example, the electric field is given as: $\vec{\mathcal{E}}(\vec{r},t) = Re[\vec{E}(\vec{r})e^{j\omega t}]$. Maxwell's equation become:

$$\nabla \cdot \vec{E}(\vec{r}) = \frac{\vec{\rho}_e(\vec{r})}{\epsilon_0} \tag{3.14}$$

$$\nabla \cdot \vec{H}(\vec{r}) = 0 \tag{3.15}$$

$$\nabla \times \vec{E}(\vec{r}) = -j\omega\mu_0 \vec{H}(\vec{r}) \tag{3.16}$$

$$\nabla \times \vec{H}(\vec{r}) = \vec{J}_e(\vec{r}) + j\omega\epsilon_0 \vec{E}(\vec{r}) \tag{3.17}$$

As the region of interest is the is the far field, the solution of the Maxwell's equations gives the following functions, for an antenna of finite volume V_0 with electric current distribution $\vec{J}_e(\vec{r_0})$:

$$\vec{E} = \frac{-jk_0e^{-jk_0r}}{4\pi r}\vec{e_r} \times \int_{V_0} \vec{J_e}(\vec{r_0})e^{jk_0(\vec{e_r},\vec{r_0})}dV_0 \tag{3.18}$$

$$\vec{H} = \frac{-k_0^2e^{-jk_0r}}{-j\omega\epsilon_0 4\pi r}\vec{e_r} \times \vec{e_r} \times \int_{V_0} \vec{J_e}(\vec{r_0})e^{jk_0(\vec{e_r},\vec{r_0})}dV_0 \tag{3.19}$$

In addition, the relation between electric and magnetic field is $\vec{E} = Z_0\vec{H} \times \vec{e_r}$ with $Z_0 = \sqrt{\frac{\mu_0}{\epsilon_0}}$ which is approximately 377Ω, known as the impedance of free space. The vector is given as $\vec{e_r} = \vec{r}/r$ with $r^2 = x^2 + y^2 + z^2$. Also, inside the integral, the symbolism of $(\vec{e_r}, \vec{r_0})$ corresponds to a phase difference between source point Q $(x0, y0, z0)$ and the origin $(0, 0, 0)$. Finally, the Poinitng vector is found in 3.20. Is is clear that the fields have a radial dependence and the energy flows at the direction of $\vec{r}$.

$$\vec{S}(\vec{r}) = \frac{1}{2Z_0}|\vec{E}|^2\vec{e_r} \tag{3.20}$$

3.3.2 Electric dipole antenna

There are many types of antennas, which could be analyzed regarding the theory that was explained in this chapter. At this point there will be a brief reference of the elementary antenna, called *electric dipole* in order to have an example and get a more practical comprehension. Electric dipole is a very small linear antenna, with length much smaller than the free space wavelength λ_0. The current distribution $\vec{J_e}$ of a dipole with length l and total current I_0, is given with the help of the delta function [4]:

$$\vec{J_e}(\vec{r}) = I_0l\delta(x)\delta(y)\delta(z)\vec{e_z} = I_0l\delta(\vec{r})\vec{e_z}$$

The current is distributed along the length of the antenna, which is located on the z-axis. For the far field, the electric and magnetic fields, are found below:

$$\vec{E} = E_\theta\vec{e_\theta} = \frac{jk_0I_0le^{-jk_0r}}{4\pi r}sin\theta\vec{e_\theta}$$
$$\vec{H} = H_\phi\vec{e_\phi} = \frac{jk_0I_0lZ_0e^{-jk_0r}}{4\pi r}sin\phi\vec{e_\phi}$$

The fields are perpendicular to each other, while the direction of Poynting vector is radial:

$$\vec{S}(\vec{r}) = \frac{1}{2}\frac{jk_0^2Z_0(I_0l)^2e^{-jk_0r}}{(4\pi r)^2}sin^2\theta\vec{e_r}$$

From this relation, we can conclude that the dipole does not radiate uniformly in all directions,e.g. for $\theta = 0$, energy flux is eliminated. The parameters of the antenna such as radiation pattern or directivity are explained in the next paragraphs, but first it is important to calculate the total power radiated by the antenna:

$$P_t = \frac{k_0 Z_0 (I_0 l)^2}{12\pi}$$

According to Poynting vector, the normalized radiation pattern is calculated below and figure 3.6 shows a 2D graphical representation:

$$F(\theta) = \frac{P(\theta)}{P(\pi/2)} = sin^2\theta$$

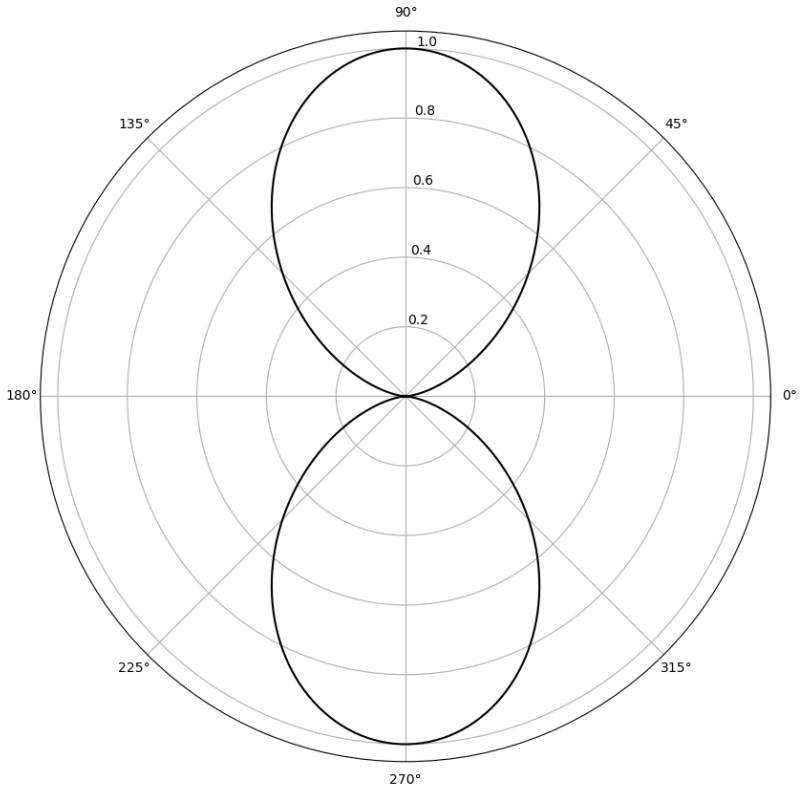

Figure 3.6: Normalized radiation pattern of an electric dipole created in python ($\theta = 0$ coincides with the positive z-axis)

Next, we can compute the directivity function:

$$D(\theta) = \frac{P(\theta)}{P_t/4\pi} = \frac{3}{2} sin^2\theta$$

Note that in the parameters there was not the variable of ϕ the Poynting vector or power function did not have such a dependency. The electric dipole can have a length of $0.01\lambda_0$ while its impedance consists of only a real-ohmic part. The resistance of a dipole is poor (e.g. $R = 0.08\Omega$), a fact that makes it unsuitable for matching with a transmission line. For this reason it used in applications like low-frequency radio-astronomy [15].

3.4 Microstrip - Patch antenna

At the last part of this chapter, after the brief explanation of the elementary dipole antenna, we go on, with a relatively modern invention. The *microstrip antenna* (MSA) or *patch antenna* has been a major component of today's wireless communications. It was invented in 1955, although, since the recent years it was not so popular [7]. The geometry of the MSA is not so common. It consists of a dielectric substrate, which is "sandwiched" between a conducting plane on the bottom side and a metal patch on top. The dielectric substrate has a certain thickness h and a dielectric constant ϵ_r. The conducting or ground plane, covers the whole of the bottom side, while the patch comes in various shapes, usually rectangular or circular. Also, the fabrication of such structures is achieved with the help of printed circuit board (PCB) techniques, which are cheap and offer high accuracy, reaching below $100\mu m$ [4]. Microstrip antennas are *resonant* antennas, meaning that at specific frequencies they become purely resistive and it can be matched with a transmission line.

In order to feed an MSA, usually a microtstrip line is connected to the metal patch, where at the other side of the line there is a circuitry. Another way might be a coaxial feed or a direct feed by connecting a signal source across the microstrip line and the ground plane [6].For a better comprehension, figure 3.7 shows a microstrip antenna with a rectangular patch. For such an antenna, the radiation properties are determined by what is called *fringing fields*. When the antenna is fed, EM waves start coupling from the patch to the ground, inside the dielectric material. Although, at the edges the waves travel from the air and then reach the ground. This phenomenon is responsible for the radiation of a rectangular MSA. Figure 3.8 depicts the fringing fields of the structure.

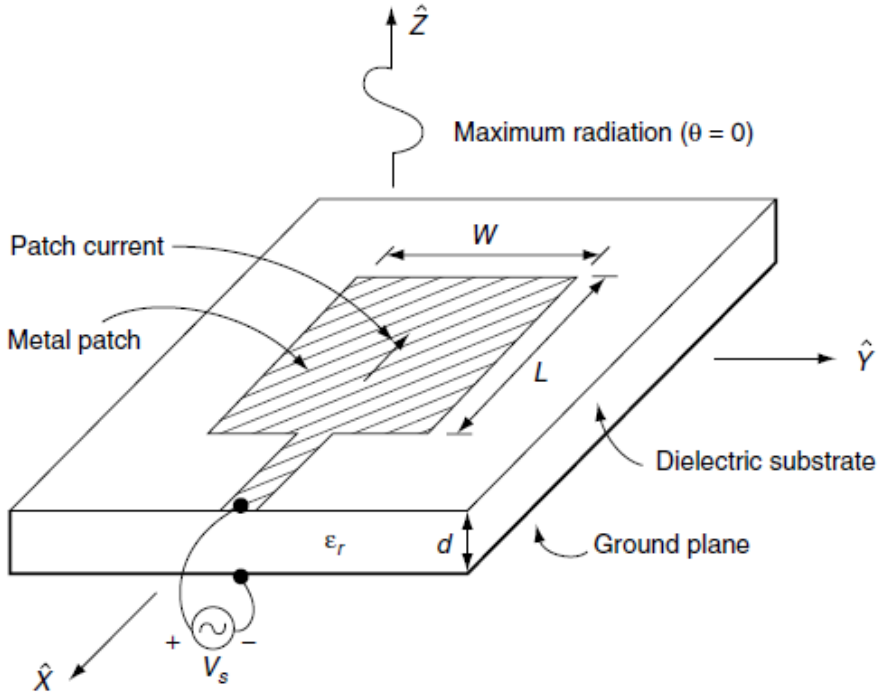

Figure 3.7: Geometry of a Rectangular Microstrip Antenna. It consists of a rectangular metal patch on a dielectric substrate and is excited by a voltage source across the metal patch and the bottom ground plane of the substrate. The microstrip antenna produces maximum radiation in the broadside direction ($\theta = 0$), with ideally no radiation along the substrate edges ($\theta = 90$) [6]

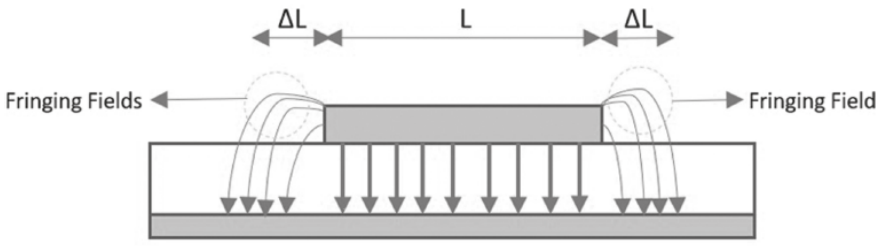

Figure 3.8: Fringing fields of a rectangular patch antenna [7]

In order to determine the radiation properties of an MSA, we will use the tequiche called *cavity model* for a circular shaped patch, although there can be and other methods such as the transmission line model or numerical methods like the Method of Moments(MoM) [4].Unlike rectangular MSA, circular does not create fringing fields. For the cavity model, imagine a cylinder that is created, on top with a circular patch with $\rho = \alpha$, at the bottom the ground

plane and between those metals a homogeneous dielectric material. This cylinder is called cavity. The fields are concentrated inside this cavity, while due to the small thickness of the dielectric ($h << \lambda_0$) there is no z coordinate dependency inside. Outside the cylinder the electric field is on the z directions, $\vec{E} = \vec{E_z}\vec{e_z}$, while the magnetic field will be orthogonal to the side walls of the cavity. This is because, the electric current distribution $\vec{J_e}$ is along the edge of the circle($\rho = \alpha$), which is the edge of the patch. So for the magnetic field $\vec{H} = \vec{J_e} \times \vec{e_z}$.

According to the theory of *Modern Antennas and Microwave Circuits* [4] and with the help of cylindrical coordinates (ρ, ϕ, z), the electric field inside the cavity is given by the equation:

$$E_z = E_0 J_n(k\rho)cos(n\phi) \tag{3.21}$$

where $J_n(k\rho)$ is a first kind Bessel function with order n and $k = k_0\sqrt{\epsilon_0}$ the substrate wave number. The other electric field's components are zero($E_\rho = E_\phi = 0$). In addition for the magnetic field, $H_z = 0$ and:

$$H_\rho = \frac{n}{j\omega\mu_0\rho}E_0 J_n(k\rho)sin(n\phi) \tag{3.22}$$

$$H_\phi = \frac{n}{j\omega\mu_0}E_0\frac{\partial J_n(k\rho)}{\partial\rho}cos(n\phi) \tag{3.23}$$

The radiation pattern as well as the other parameters of an MSA require mathematical tools, which cannot be analytically explained at this point. First, in the far-field region, the electric field components are given as below:

$$E_\theta = \frac{j^n ahk_0 E_0 J_n(ka)e^{-jk_0 r}}{2r}cos(n\phi)(J_{n+1}(k_0 asin\theta) - J_{n-1}(k_0 asin\theta)) \tag{3.24}$$

$$E_\phi = \frac{j^n ahk_0 E_0 J_n(ka)e^{-jk_0 r}}{2r}cos(\theta)sin(n\phi)(J_{n+1}(k_0 asin\theta) + J_{n-1}(k_0 asin\theta)) \tag{3.25}$$

where for the fundamental mode they become:

$$E_\theta = \frac{jahk_0 E_0 J_1(ka)e^{-jk_0 r}}{2r}cos(\phi)(J_2(k_0 asin\theta) - J_0(k_0 asin\theta)) \tag{3.26}$$

$$E_\phi = \frac{jahk_0 E_0 J_1(ka)e^{-jk_0 r}}{2r}cos(\theta)sin(\phi)(J_2(k_0 asin\theta) + J_0(k_0 asin\theta)) \tag{3.27}$$

In this manner, the normalized radiation pattern takes the form seen in 3.28:

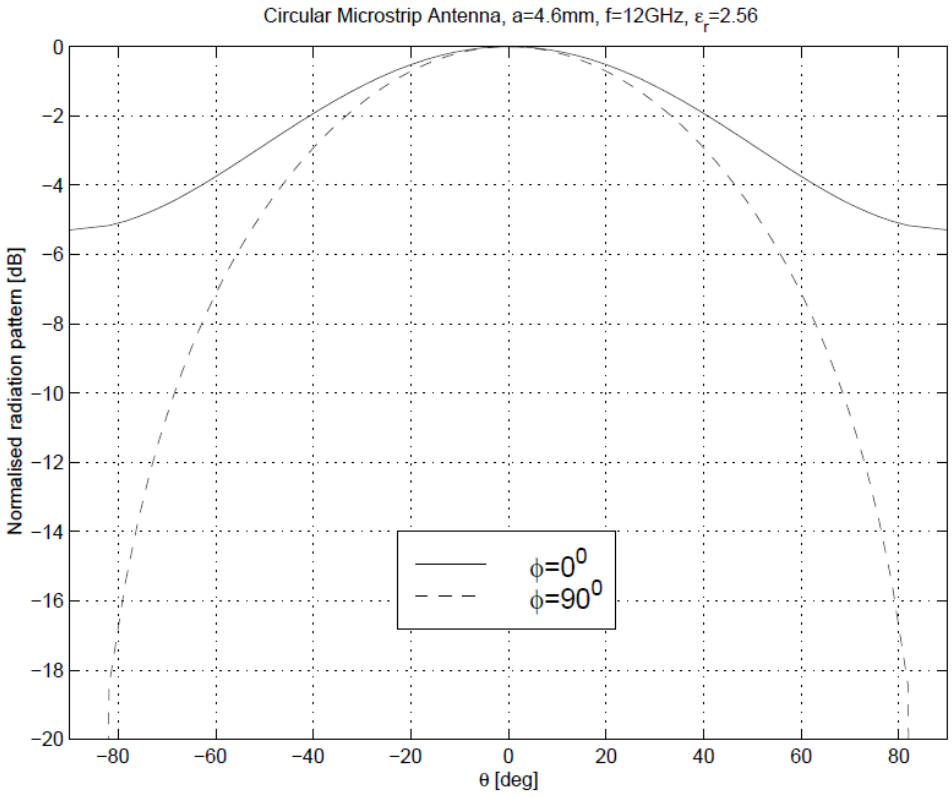

Figure 3.9: Normalized radiation pattern of circular MSA

$$F(\theta,\phi) = \frac{|E_\theta(\theta,\phi)|^2 + |E_\phi(\theta,\phi)|^2}{|E_\theta(\theta_0,\phi_0)|^2 + |E_\phi(\theta_0,\phi_0)|^2} \tag{3.28}$$

with the set (θ_0, ϕ_0) the points where the maximum values of those functions occur. The figure at 3.9 shows an example of a circular's patch normalized radiation pattern operating at $12GHz$.

As it was mentioned previously, MSA's are resonant antennas. At resonant frequencies the antenna can be matched with a transmission line with characteristic impedance 50Ω. It is also important to mention another parameter of the antenna which is the bandwidth (BW). Bandwidth is the range of frequencies where the antenna can operate properly. In addition, BW depends on the design of the structure, like the dielectric substrate thickness. A larger bandwidth, which is significant for modern systems, can be obtained by using stacked patches or by using a resonant slot feed in the ground plane [16].

Despite the low gain or the large ohmic losses, microstrip antennas come in small size, low cost and can operate at multiple frequencies. They are suitable for various applications like

GPS, radar systems and satellite communications [7], while they have played a significant role in the development of the 5^{th} generation of wireless systems, as they are a main component of smart antennas like phased arrays.

Chapter 4

Phased Arrays

4.1 Introduction

Phased arrays can also be labeled as smart antennas, as they have the ability to steer the beam at the desired direction. They are not a new innovation because they have been deployed since 1970 for military purposes. They consist of small antennas with low gain, structured in a linear or planar shape. This small elements could either be dipole antennas or microstrip antennas. By manipulating the phase and amplitude of each element, the radiation can be sent to the direction we want, and that's why they are named Phased Arrays. In addition, in modern wireless systems they have the ability to communicate with more than one target simultaneously. So, combined with the fact that a phased array can consist of MSA elements, there can be a system which is characterized by low cost, adjustable size and useful for many applications.

One of those applications is the future mm-Wave 5G wireless communication system which is being deployed the last few years. The beamsteering capabilities along with the high gain of the antenna makes phased arrays very suitable for modern structures. A significant parameter of today's telecommunication systems is the MIMO technique, that stands for Multiple-Input-Multiple-Output, while for 5G technologies is evolved in mMIMO (massiveMIMO). In simple words, MIMO is the act of sending various packets of information to numerous targets, operating at the same frequency. Consequently, MIMO configuration plays a fundamental role for the standardization of the 5^{th} generation systems [17].

4.2 Linear Phased Arrays

In theory, transmit and receive antennas can be identical due to reciprocity, however in practical implementation, there are differences on the electronics of the elements. A linear array, consists of K isotropic radiators, that are located along the x axis, with the first antenna ($k = 1$) at the origin of the coordinate system, $(x, y, z) = (0, 0, 0)$. The single elements distance is d_x, while each of them is connected to a circuit which performs the complex weighting of the received signals s_k. In other words, what is meant by complex weighting is a multiplication with a complex coefficient $a_k = |a_k|e^{-j\psi_k}$, with $|a_k|$ known as *taper* and $-\psi_k$ is the phase shift.

Suppose there is a linear phased array functioning at the receive mode. A wave reaches the antenna with a certain angle θ_0 and s_k is the signal of the k element. $s_k = e^{-jk_0(k-1)d_x sin\theta_0}$, and can be understood as a voltage along a circuit connected to the port of the antenna, or as a complex amplitude of a wave that is guided along a transmission line, which is also be connected to each antenna. The signals are then added to a *summing network* and the total received signal is given as:

$$S(\theta_0) = \sum_{k=1}^{K} |a_k|e^{-j[k_0(k-1)d_x sin\theta_0 - \psi_k]}$$

$S(\theta_0)$ is the response of the received signal and is referred as *array factor*. At figure 4.1 it is shown a graphical representation of a linear phased array connected to a summing network. The array factor is a periodical function with λ_0/d_x period and its maximum occurs when $\psi_k = k_0(k-1)d_x sin\theta_0$, so when the applied phase is manipulated by the electronics, then the direction (θ_0) of the beam does too, resulting in the desired outcome of steering the main lobe. Finally, with the introduction of the variables $u = sin\theta$ and $u_0 = sin\theta_0$ we get the the form 4.1 of the array factor which will be used in the next sections.

$$S(u) = \sum_{k=1}^{K} |a_k|e^{-j[k_0(k-1)d_x(u-u_0)]} \tag{4.1}$$

4.2.1 Amplitude Tapering and Pattern Synthesis

The way the pattern synthesis of a phased array is created is very important, as factors like the size of sidelobes or how narrow the beam is, affect the system parameters (directivity, gain, etc) of the radiating element [17]. As the array factor 4.1 is a periodic function, more

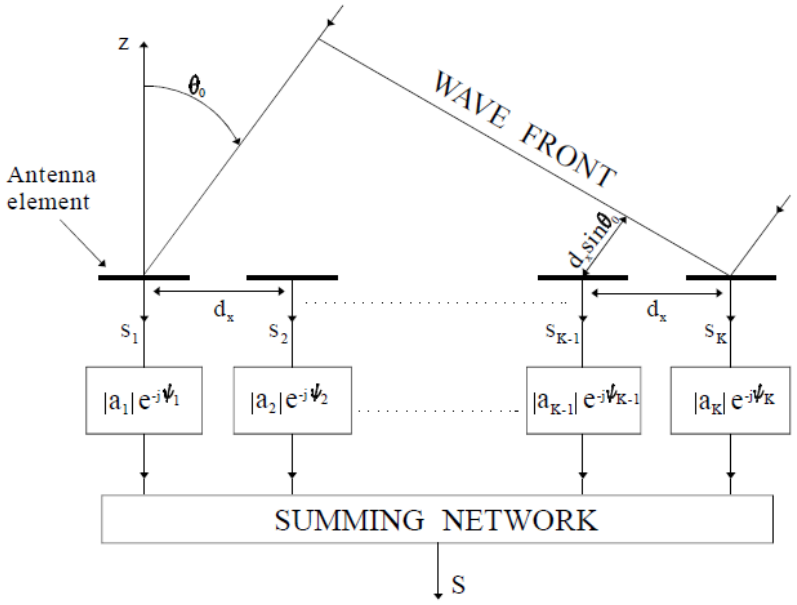

Figure 4.1: Linear phased array with K antenna elements connected to a summing network [4]

than one local maximas will occur, with the largest of those values located at direction θ_0. That is when the sidelobes are created, as described and in chapter 3. The spacing d_x among the elements of the array can define the location of sidelobes w.r.t the main direction. When the variable of u is expressed as $k_0(k-1)d_x(u_m - u_0) = 2\pi m$ it gives the appearance of sidelobes, with m an integer. Additionally, when the spacing $d_x \leq \lambda_0/2$ is applied, sidelobes can be avoided [4].

In order to define the radiation pattern for a phased array, amplitude tapering plays a major role. There are various techniques to achieve this, which give us different quality outcomes regarding the system parameters. The normalized radiation pattern is given according to the equation of 4.2:

$$F(u) = \frac{|S(u)|^2}{|S(u)|^2_{max}} \tag{4.2}$$

By applying $|a_k| = 1$ for every k, then we have the uniform amplitude tapering, and the 4.1 becomes:

$$S(u) = \sum_{k=1}^{K} e^{-j[k_0(k-1)d_x(u-u_0)]}$$

and the normalized pattern will eventually be:

$$F(u) = \left(\frac{sin(Kk_0d_x(u-u_0)/2}{Ksin(k_0d_x(u-u_0)/2} \right)^2$$

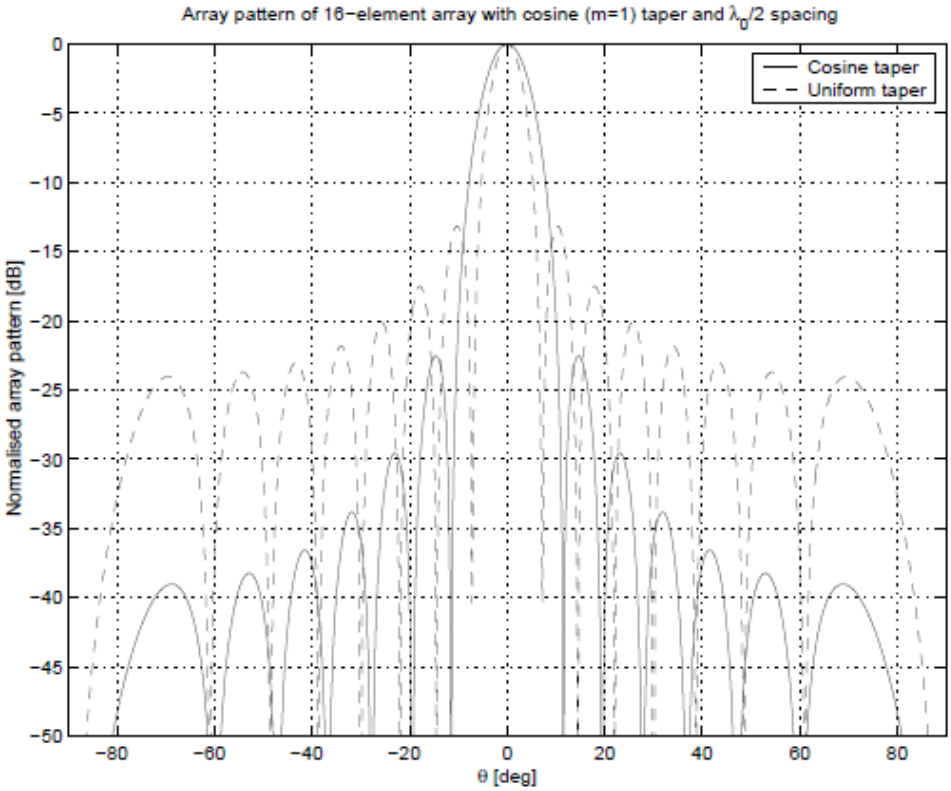

Figure 4.2: Normalized radiation pattern of uniform and cosine (m=1) tapering [4]

with K the number of antennas of the linear array [17]. Another tapering method is the cosine tapering where $|a_k| = h + (1-h)cos^m(\frac{x_k}{Kd_x})$ where x_k is the coordinate of the elements on x axis, and h provides to use an offset (Pedestal), while m is an integer. When $h = 1$ is applied, we get the uniform tapering. Usually $m = 1$ or $m = 2$ is applied, getting cosine and square-cosine weighting respectively. The cosine taper offers lower sidelobes compared to the uniform tapering, a considerable improvement for the array as seen in figure 4.2, for an array of 16 antennas and spacing $\lambda_0/2$. Other commonly used methods are the Taylor taper and the Dolph-Tchebycheff taper. Taylor taper creates a monotonic decrease of the sidelobes and Dolph-Tchebycheff taper gives a constant level for the sidelobes.

Next, the pattern synthesis of an array, or the way to control the main beam and sidelobes, offer the possibility to create narrow-beam and low-sidelobe array factors. A frequently used procedure is the Schelkunov's (Schelkunoff's) Form [17], where the array factor $S(u)$ takes the following polynomial form:

$$S(z) = \sum_{k=1}^{K} |a_k| z^{k-1} \tag{4.3}$$

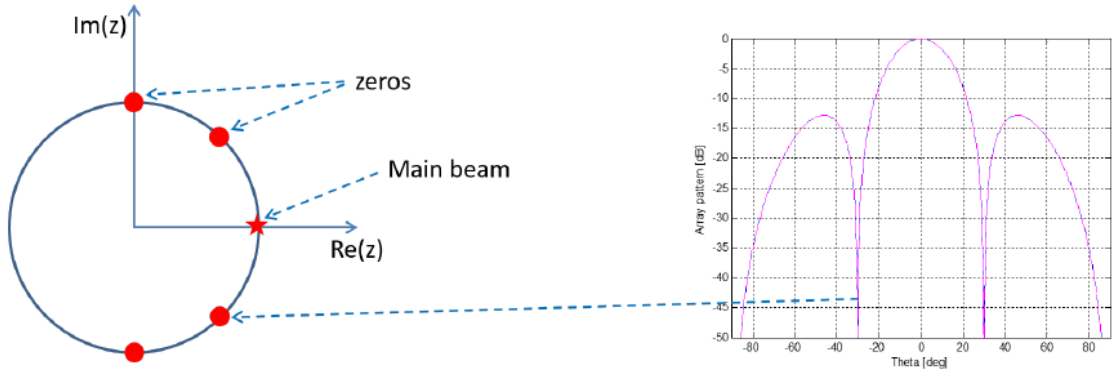

Figure 4.3: Graphical representation of Schelkunov's polynomial zeros on the complex plane (left) with respect to the normalized radiation pattern (right) [4]

or in the form of product

$$S(z) = a_K \prod_{k=1}^{K-1} (z - z_k) \tag{4.4}$$

with $z = e^{jk_0 d_x sin\theta}$ and $a_k = |a_k| e^{-jk_0 d_x sin\theta_0}$. It is clear that $(z_1, z_2, .., z_{K-1})$ correspond to the zeros of the Schelkunov's polynomial, meaning null-locations of the radiation pattern as seen in figure 4.3.

4.2.2 Directivity and Beamwidth

In chapter 3, there was an description of antenna parameters such as directivity. It was defined as the concentration of power to a specific direction w.r.t. other direction. Now, suppose that the beam has a θ_0 direction, then we have:

$$D(\theta_0) = \frac{P(\theta_0)}{P_t/4\pi} = \frac{4\pi |S(\theta_0)|^2}{\int_{V_\infty} |S(\theta)|^2 d\Omega} \tag{4.5}$$

P_t is the total radiated power and $d\Omega$ is the differential solid angle. As previously, we set $u = sin\theta$ and consequently $du = cos\theta d\theta$ and the directivity of a linear array, with $\theta_0 = 0$ becomes [17]:

$$D = \frac{\left(\sum_{k=1}^{K} |a_k|\right)^2}{\sum_{k=1}^{K} |a_k|^2} \tag{4.6}$$

For example, the directivity of a uniform tapered array($|a_k| = 1$) is $D = K$. If $K = 1000$,

$D = 10log_{10}(1000) = 30dB$. If $|a_k| \leq 1$ the directivity is reduced according to the factor:

$$n_{tap} = \frac{\left(\sum_{k=1}^{K} |a_k|\right)^2}{K \sum_{k=1}^{K} |a_k|^2}$$

and directivity becomes : $D = n_{tap}K$ [4].

Another antenna parameter is the half power beam width, which is an angle that indicates the region where the 50% of the power is concentrated. For a uniformly tapered linear array this angle is [4]:

$$\theta_{HPBW} = \frac{0.8858\lambda_0}{Kd_x cos\theta_0}$$

4.3 Physical Antenna Structures - Mutual Coupling

What has been explained up to this point, has to do with a more theoretical approach of phased arrays. In practice, the elements of an array cannot be isotropic radiators as such structures exist only in theory. Phased arrays can be built up with physical antennas like electric dipoles or MSA, which individually have a broad beam width, so finally we can get a broader scan angle for the array. In this case, there a little change in the array factor [4]:

$$\vec{S}(u) = \vec{f}(u) \sum_{k=1}^{K} |a_k| e^{-j[k_0(k-1)d_x(u-u_0)]} \tag{4.7}$$

where $f(\vec{u})$ is called element factor and describes the electric field of an individual element. The element factor, as the antennas are of the same type, eventually can be written outside the summation of the signals.

Next, another phenomenon concerning the structure of a phased array is the so-called *mutual coupling*. In simple words, mutual coupling is the electromagnetic interaction between the individual elements. As a result, the element pattern or the input impedance of each antenna is affected. In order to investigate this phenomenon, we will use the method of microwave networks. Transmission lines are connected to the input port of each element and they are used to propagate waves at the them. A wave of complex amplitude a_k arrives a port k, while a reflected wave of amplitude b_k travels to the opposite side. A process to measure the complex amplitudes was discussed in chapter 3, the Vector Network Analyzer (VNA). For an example of a 2-port network the waves' relation is given by:

$$\begin{bmatrix} b_1 \\ b_2 \end{bmatrix} = \begin{bmatrix} S_{11}\ S_{12} \\ S_{12}\ S_{22} \end{bmatrix} \begin{bmatrix} a_1 \\ a_2 \end{bmatrix}$$

where:

- S_{11} is the reflection coefficient at port 1 when the second is terminated by a matched load
- S_{22} the reflection coefficient at port 2 when port 1 is terminated
- $S_{12} = S_{21}$ as reciprocity is applied, are the coupling coefficients of the among the antennas

In case a phased array is used for transmission the total reflected signal at each port is defined as:

$$R_k^{act}(u_0) = \frac{1}{a_k} \sum_{i=1}^{K} S_{ki} a_i(u_0)$$

R_k^{act} is called also active reflection coefficient. a_i is the excitation coefficient as defined in 4.2. The power or scan loss for every element is given as: $L_k = 1 - |R_k^{act}|^2$, describes the reduction of the antenna gain. Another equation for the active reflection coefficient is:

$$R_k^{act}(u_0) = \frac{Z_k^{act}(u_0) - Z_0}{Z_k^{act}(u_0) + Z_0}$$

$Z_0 = 50\Omega$, and is the input impedance at the port. Z_k^{act} is the active input impedance defined as:

$$Z_k^{act}(u_0) = \frac{V_k}{I_k} = \frac{1}{I_k} \sum_{i=1}^{K} Z_{ki} I_i$$

where V_k and I_k the voltage and current at k port, and Z_{ki} the mutual impedance of the elements.

Chapter 5

Simulation of Millimeter Wave Length Antennas

The simulation of modern systems and physical phenomena, has become a critical field of the today's engineering industry. For the sake of antenna and electromagnetic theory and applications, there are numerous tools which can give a precise simulations, which reduce the cost of having to built an infrastructure. Such tools are CST, HFSS and Momentum/ADS. On the other hand, python, Matlab and C++ offer modules and libraries designed for this purpose.

In this thesis there is a theoretical approach of the millimeter wave length antennas for 5G applications, and below I will show the results of a python simulation of those antenna, more specific of linear phased arrays, while in the second subsection there will be a more integrated example according to ANSYS's simulation tools' white paper [18].

5.1 Simulation

The radiation properties that were introduced in the previous section [4] described tapering methods, which gave different results regarding the sidelobes as well as the directivity and the beamwidth. For the sake of this design, omnidirectional antennas were used which could be a dipole or a microstrip patch antenna. The first simulation [5.1][5.2] depicts a uniform tapered linear array of 4 elements and spacing $\lambda_0/2$. The directivity is $6.020db$ as seen in 5.3 and the half power beamwidth is 25.376^o. The first sidelode is $13db$ lower than the main lobe.

Next, at figures 5.4- 5.6, the simulation is now with a 16 element array at $f = 28Ghz$.

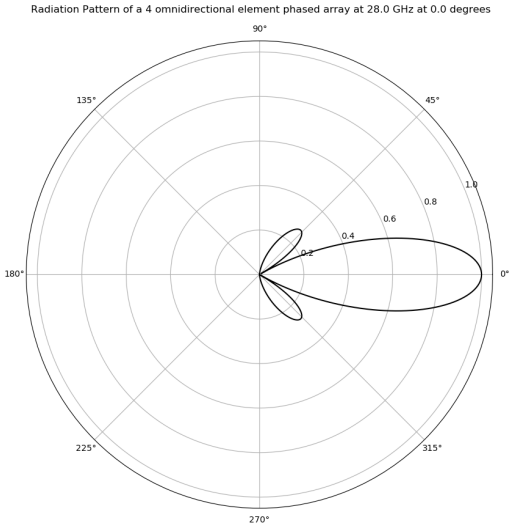

Figure 5.1: Radiation pattern of a 4 element linear array with uniform tapering,with $\theta_0 = 0$ and $dx = \lambda_0/2$ at $f = 28GHz$

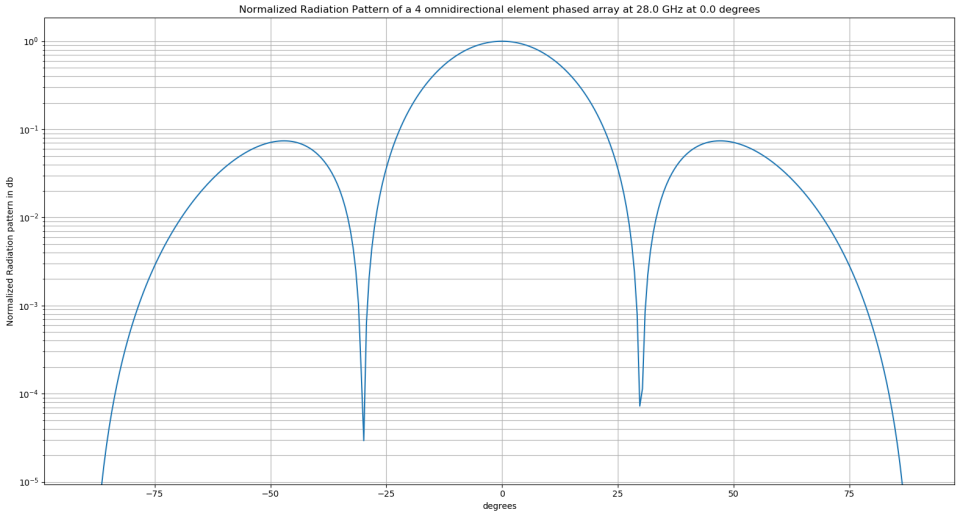

Figure 5.2: Normalized radiation pattern of a 4 element linear array with uniform tapering, with $\theta_0 = 0$ and $dx = \lambda_0/2$ at $f = 28GHz$

```
Half Power Beam Width is at 25.37630074634416 degrees
Directivity is 6.020599913279624 dB
```

Figure 5.3: Directivity and HPBW of a 4 element linear array with uniform tapering, with $\theta_0 = 0$ and $dx = \lambda_0/2$ at $f = 28GHz$

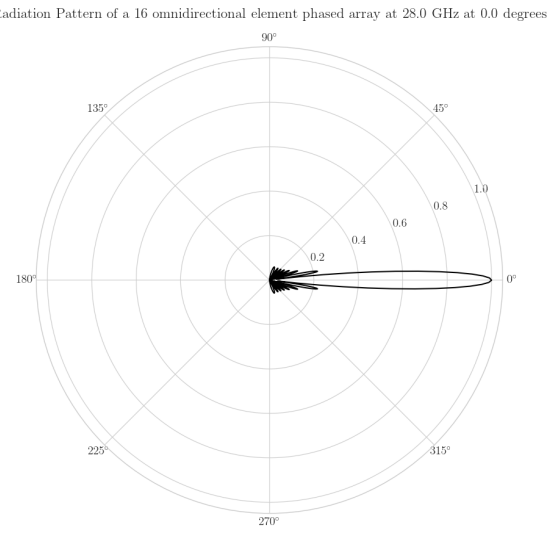

Figure 5.4: Radiation pattern of a 16 element linear array with uniform tapering, with $\theta_0 = 0$ and $dx = \lambda_0/2$ at $f = 28GHz$

As we can see from the radiation pattern the beam is narrower ($\theta_{HPBW} = 6.344^o$) and the level but the sidelobes haven't reduced as they are at $-13.2db$ like previously. However, the directivity shows a better performance at $12.041db$. Getting a narrower beam, increases the performance of the system, thus making the smart antenna more suitable.

When square cosine taper is applied [5.7- 5.8], it is very clear that the sidelobes pop up at a lower level ($-30db$) although, the directivity is not so good, as the beam is broader.

Going on, for the same linear array of 16 elements, we apply a phase shift of $\theta_0 = 40^o$ for uniform and square cosine taper methods. Figures [5.9- 5.11] show the results.

It is clear that the performance of the phased array depend on several factors like:

- Type of antenna
- Tapering
- Antenna spacing
- Number of elements

while each of those techniques have their pros and cons. A uniform tapered array give higher sidelobes compared to square cosine taper, but at the second case creates broader beams, reducing the directivity. The spacing and the number of elements affect the width of the

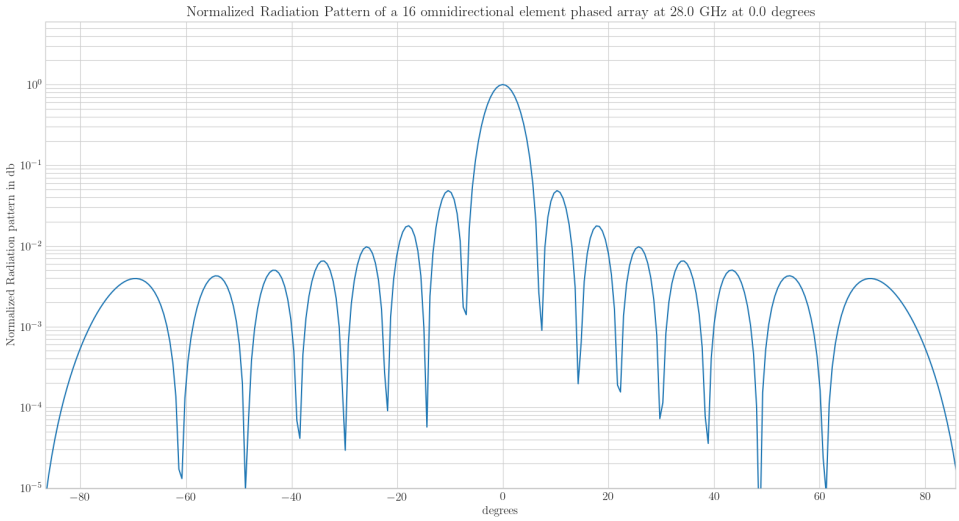

Figure 5.5: Normalized radiation pattern of a 16 element linear array with uniform tapering, with $\theta_0 = 0$ and $dx = \lambda_0/2$, at $f = 28GHz$

```
Half Power Beam Width is at 6.34407518658604 degrees
Directivity is 12.041199826559248 dB
```

Figure 5.6: Directivity and HPBW of a 16 element linear array with uniform tapering, with $\theta_0 = 0$ and $dx = \lambda_0/2$ at $f = 28GHz$

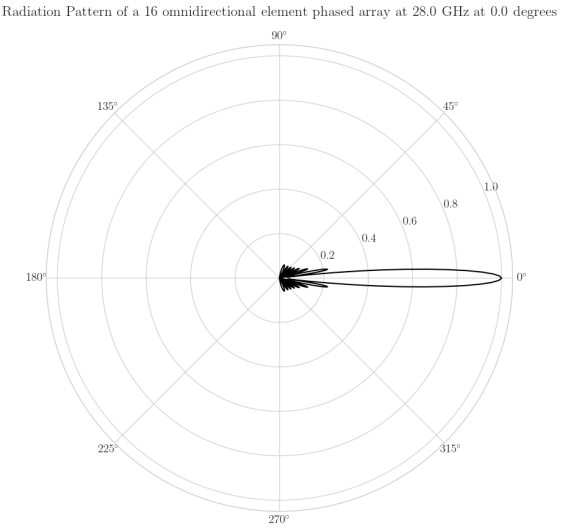

Figure 5.7: Radiation pattern of a 16 element linear array with square-cosine tapering, with $\theta_0 = 0$ and $dx = \lambda_0/2$ at $f = 28GHz$

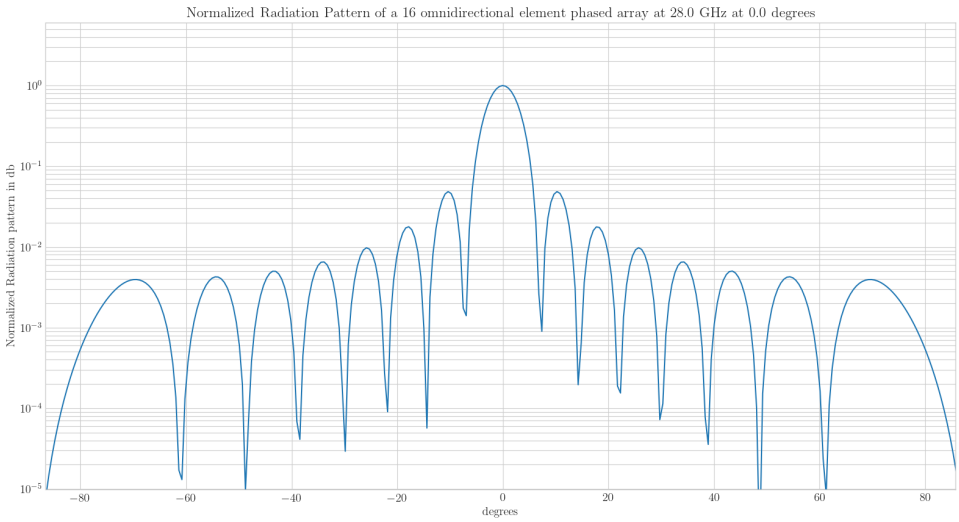

Figure 5.8: Normalized radiation pattern of a 16 element linear array with square-cosine tapering, with $\theta_0 = 0$ and $dx = \lambda_0/2$ at $f = 28GHz$

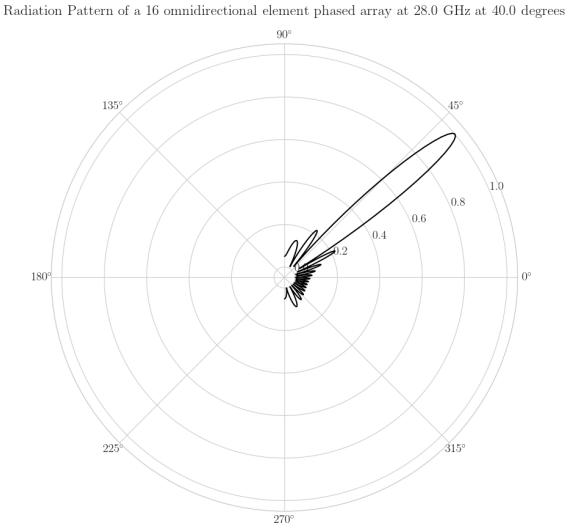

Figure 5.9: Radiation pattern of a 16 element linear array with uniform tapering, with $\theta_0 = 40$ and $dx = \lambda_0/2$ at $f = 28GHz$

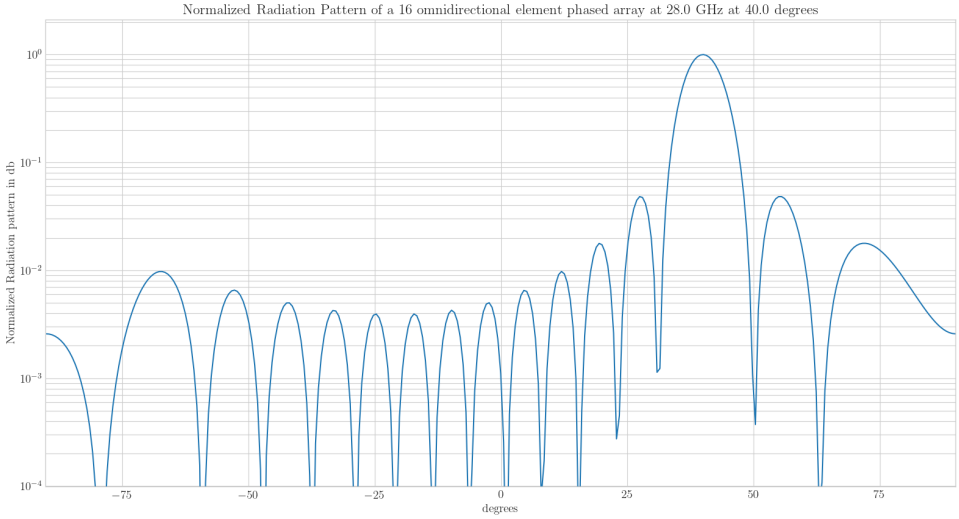

Figure 5.10: Normalized radiation pattern of a 16 element linear array with uniform tapering, with $\theta_0 = 40$ and $dx = \lambda_0/2$, at $f = 28GHz$

```
Half Power Beam Width is at 8.281601992641454 degrees
Directivity is 12.041199826559248 dB
```

Figure 5.11: Directivity and HPBW of a 16 element linear array with uniform tapering, with $\theta_0 = 40$ and $dx = \lambda_0/2$ at $f = 28GHz$

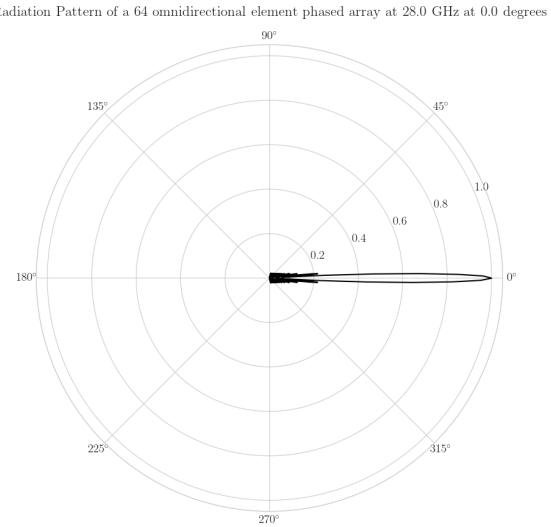

Figure 5.12: Radiation pattern of a 64 element linear array with uniform tapering, with $\theta_0 = 0$ and $dx = \lambda_0/2$ at $f = 28GHz$

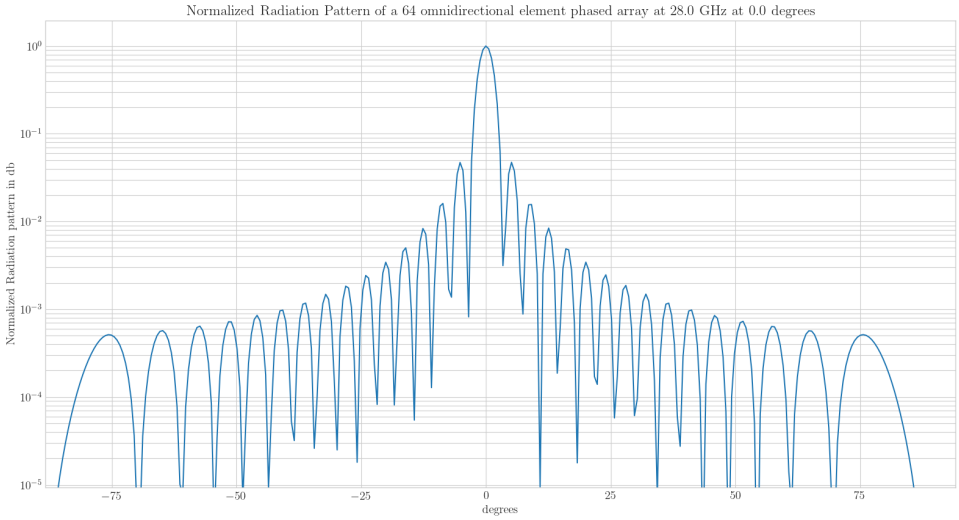

Figure 5.13: Normalized radiation pattern of a 64 element linear array with uniform tapering, with $\theta_0 = 0$ and $dx = \lambda_0/2$, at $f = 28GHz$

```
Half Power Beam Width is at 1.58601879664651 degrees
Directivity is 18.06179973983887 dB
```

Figure 5.14: Directivity and HPBW of a 64 element linear array with uniform tapering, with $\theta_0 = 0$ and $dx = \lambda_0/2$ at $f = 28GHz$

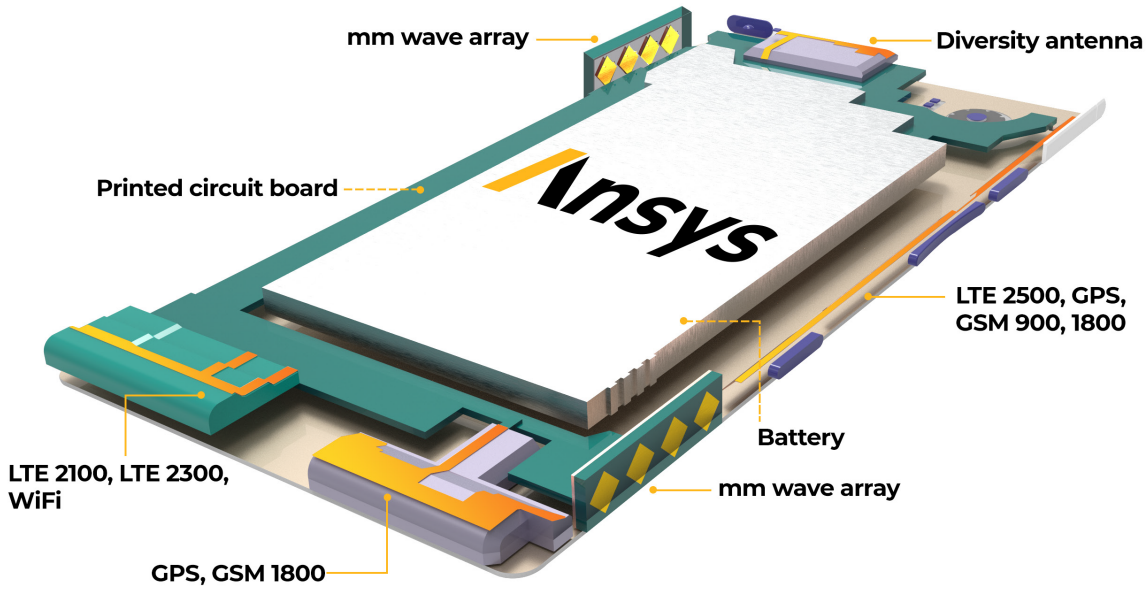

Figure 5.15: Internal details of a Smartphone

beam, the height of sidelobes and the directivity.

Finally, the infrastructure's performance is affected also from the mutual coupling between the elements. The python scripts which where developed for this chapters simulations are listed in Annex A.

5.2 Integrated Millimeter-Wave Array for User Equipment

According to ANSY's white paper *How to Design User Equipment Antenna Systems for 5G Wireless Networks* [18], phased arrays are used for typical User Equipment (UE) like smartphones, tablets, medical devices, and smartwatches etc. In this case we will see how phased are integrated on a smartphone as shown in 5.15. Smartphones capable of 5G connectivity should be able to support and other services such as LTE, GSM and GPS connectivity. The specific UE consists of 2 linear phased arrays, 4×1, more specific mm wave arrays.

Another example of integrated millimeter-wave Array for UE is shown in 5.16. The frequency band of interest for the array is 26 - $28.5GHz$. These frequencies belong to the Ka-band mm-wave sub-bands that are being considered for 5G (bands n257, n258, n260 and n261). Each element of the mm-wave array is a microstrip patch with two probe feeds.

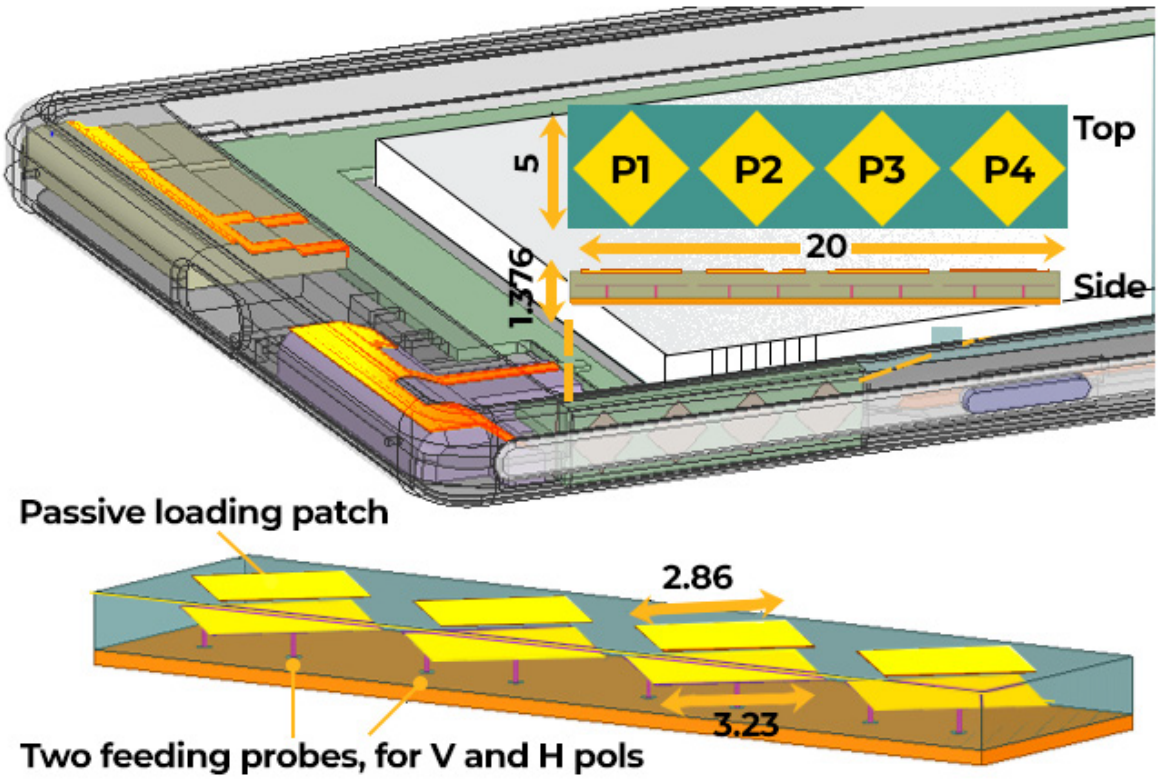

Figure 5.16: A 4×1 patch array with dual polarization (V, H), substrate Roger RT/Duriod 5870 (units: mm): stacked patch for bandwidth

The substrate is $1.376mm$ thick and assigned the material Roger RT/Duroid 5870 (dielectric constant = 2.33, dielectric loss tangent = 0.0012). A passive parasitic stacking patch is added to improve the operational bandwidth.

Each microstrip patch element has two feeds, and supports both vertical (V) as well as horizontal (H) polarizations. Each antenna is optimized to operate at the defined band with a reasonable return loss of less than $-10dB$ ($S11 < -10dB$). On placing the individual antennas in succession along a straight line, an array is generated. The array is then integrated into the phone. At various stages of the design, from the initial element to the array and its final integration onto the phone, it is important to properly tune the antenna. Tuning the antenna and the array improves their efficiency and ensures that the electronics within the device and its housing do not decrease the array's performance.

Bibliography

[1] Oliver Lodge. *Signalling across Space without Wires: Being a Description of the Work of Hertz and his Successors*. Cambridge Library Collection - Technology. Cambridge University Press, 2013.

[2] Antennas for dummies.

[3] Side lobes in antenna systems.

[4] U. Johannsen. A.B. Smolders, H.J. Visser. *Modern Antennas and Microwave Circuits*. Cambridge Library Collection - Technology. Eindhoven University of Technology Library, 2019.

[5] Antenna polarisation by jairam sankar.

[6] Ii - antenna elements and arrays. In WAI-KAI CHEN, editor, *The Electrical Engineering Handbook*, pages 569–583. Academic Press, Burlington, 2005.

[7] Praveen Kumar Malik, Sanjeevikumar Padmanaban, and Jens Bo Holm-Nielsen. *Microstrip antenna design for wireless applications*. CRC Press, 2021.

[8] Sardiah Mae Mocorro. Pyramidal horn antenna, Nov 2017.

[9] Radio astronomy facilities.

[10] Defected ground structure microstrip antenna for wimax.

[11] Bedilu Befekadu Adela, Paul T. M. van Zeijl, Ulf Johannsen, and A. Bart Smolders. On-chip antenna integration for millimeter-wave single-chip fmcw radar, providing high efficiency and isolation. *IEEE Transactions on Antennas and Propagation*, 64(8):3281–3291, 2016.

[12] Jonathan Rodriguez. *Fundamentals of 5G Mobile Networks*. John Wiley and Sons, 2015.

[13] Patrick Marsch, Ömer Bulakçi, Olav Queseth, and Mauro Boldi. *5G system design: architectural and functional considerations and long term reseach*. Wiley, 2018.

[14] Keqian Zhang and Dejie Li. *Electromagnetic theory for microwaves and optoelectronics*. Springer, 2008.

[15] Donald Charles, J. R. Fisher, and John Dreher. *Square-Kilometer Array (SKA): background, strawman specifications, and discussion of problems that can benefit from expertise in other URSI commissions*. publisher not identified, 1998.

[16] A.B. Smolders. *Microstrip phased-array antennas : a finite-array approach*. PhD thesis, Electrical Engineering, 1994.

[17] Robert J. Mailloux. *Phased array antenna handbook*. Artech House, 2018.

[18] Designing next-gen user equipment antenna systems for 5g wireless networks.

APPENDICES

Appendix A

Python Codes

A.0.1 Uniform Tapering

```
import numpy as np
import matplotlib.pyplot as plt


c= 3e8
f = 12e9
wave_len = c/f
dx = wave_len/2
theta0 = 0
theta0 = np.deg2rad(theta0)
K = 4

k0 =2*np.pi/wave_len

#theta values from -90 to 90 degrees
theta = np.arange(-np.pi/2, (np.pi)/2, 0.01)
phi = np.arange(0, (np.pi), 0.01)

#define the variables u and u0
u = np.sin(theta)
u0 = np.sin(theta0)



S_u = np.exp(1j*(K-1)*k0*dx*(u-u0))*(np.sin(K*k0*dx*(u-u0)/2)/(K*np.sin(k0*dx*(u-u0)/
```

```
S_u1 = np.abs(S_u)

#Normalized Radiation Pattern for a uniform tapered linear array
F1 = (np.sin(K*k0*dx*(u-u0)/2)/(K*np.sin(k0*dx*(u-u0)/2)))
F = F1**2

#Directiviy and Half Power Beam Width
HPBW1 = 0.8858*wave_len / (K*dx*np.cos(theta0))
print('Half Power Beam Width is at '+str(np.rad2deg(HPBW1))+' degrees')

D = 10*np.log10(K)
print('Directivity is '+str(D)+' dB')



#plot  Radiation Pattern
plt.figure(figsize=(30, 30))
plt.axes(projection = 'polar')
plt.polar(theta ,S_u1,'-k')
plt.title(' Radiation Pattern of a '+str(K)+
          ' omnidirectional element phased array at '+str(f/1e9)+
          ' GHz at '+str(np.rad2deg(theta0))+' degrees')
plt.show()

#Normalized Radiation Pattern in dB
plt.figure(figsize=(30, 30))
NF = 10*np.log10(F)
#print(NF)
plt.grid(True, which ="both")
plt.semilogy(np.rad2deg(theta),F)



# Provide the title for the semilogy plot
plt.title('Normalized Radiation Pattern of a '+str(K)+
          ' omnidirectional element phased array at '+str(f/1e9)+
          ' GHz at '+str(np.rad2deg(theta0))+' degrees')

# Give x axis label for the semilogy plot
plt.xlabel('degrees')
```

```
# Give y axis label for the semilogy plot
plt.ylabel('Normalized Radiation pattern in db')
plt.show()
```

A.0.2 Cosine Tapering

```
import numpy as np
import matplotlib.pyplot as plt

c= 3e8
f = 28e9
wave_len = c/f
dx = wave_len/2
theta0 = 0
theta0 = np.deg2rad(theta0)
K = 16

k0 =2*np.pi/wave_len

#theta = np.arange(-np.pi/2, (np.pi)/2, np.pi/(K))
theta1 = np.arange(-np.pi/2, (np.pi)/2, 0.01)

u = np.sin(theta1)
u0 = np.sin(theta0)

#x-axis coordinate of element
xk = (K)*[0]
for k in range(K):
    xk[k]= (k)*dx

xk = np.array(xk)


#cosine taper parameters
m = 2
h = 2

ak_magn = h + (1-h)*np.cos(np.pi*xk/(K*dx))**m
```

```
ak = ak_magn*np.exp(-1j*k0*dx*u0)

z = np.exp(1j*k0*dx*u)

#Array factor or signal computation
S = []
for k in range(K):
    S.append(ak[k]*z**(k))
S = np.array(S)
S_u = np.sum(S,axis=0)



#Normalized Radiation Pattern for a square cosine tapered linear array
s = np.abs(S_u)
s_max = max(s)
S_sq =s**2
F = S_sq/s_max**2


#Directiviy and Half Power Beam Width
#HPBW = 40/np.cos(np.rad2deg(theta0))
#print('Half Power Beam Width is at '+str(np.rad2deg(HPBW))+' degrees with cosine tap

D = np.sum(ak_magn)**2/np.sum(ak_magn**2)
D_db = 10*np.log10(D)
n_tap =  np.sum(ak_magn)**2/(K*np.sum(ak_magn**2))
print('Directivity is '+str(D_db)+' dB')


#plot  Radiation Pattern
plt.figure(figsize=(30, 30))
plt.axes(projection = 'polar')
plt.polar(theta1 ,s,'-k')
plt.show()

plt.figure(figsize=(30, 30))
plt.grid(True, which ="both")
#plt.semilogy(np.rad2deg(THETA_),F_)
```

```
plt.semilogy(np.rad2deg(theta1),F)

# Provide the title for the semilogy plot
plt.title('Normalized Radiation Pattern of a '+str(K)+
          ' omnidirectional element phased array at '+str(f/1e9)+
          ' GHz at '+str(np.rad2deg(theta0))+' degrees with cosine taper')
# Give x axis label for the semilogy plot
plt.xlabel('degrees')

# Give y axis label for the semilogy plot
plt.ylabel('Normalized Radiation pattern in db')
#


plt.show()
```